sustainability

MDPI

Article

Upgrading Sustainability in Clean Energy: Optimization for Proton Exchange Membrane Fuel Cells Using Heterogeneous Comprehensive Learning Bald Eagle Search Algorithm

Ahmed K. Ali [1,*], Ali Nasser Hussain [2], Mudhar A. Al-Obaidi [3] and Sarmad Al-Anssari [4,5]

[1] Institute of Technology, Middle Technical University, Baghdad 10074, Iraq
[2] Department of Electrical Power Engineering Techniques, Electrical Engineering Technical College, Middle Technical University, Baghdad 10074, Iraq; dr_alinasser@mtu.edu.iq
[3] Technical Instructor Training Institute, Middle Technical University, Baghdad 10074, Iraq; dr.mudhar.alaubedy@mtu.edu.iq
[4] College of Engineering, Al-Naji University, Baghdad 10074, Iraq; al-anssari@alnaji-uni.edu.iq
[5] College of Engineering, University of Baghdad, Baghdad 10071, Iraq
* Correspondence: ahmed_khalid@mtu.edu.iq

Abstract

Clean energy applications widely recognize Proton Exchange Membrane Fuel Cells (PEMFCs) for their high efficiency and environmental compatibility. Accurate parameter identification of PEMFC models is essential for enhancing system performance and reliability, particularly under dynamic operating conditions. This paper presents a novel optimization-based approach called Heterogeneous Comprehensive Learning-Bald Eagle Search (HCLBES) with enhanced exploration and exploitation capabilities for the effective modeling of PEMFC. The algorithm combines the exploration strength of the Bald Eagle Search with comprehensive learning and heterogeneity mechanisms to achieve a balanced global and local search space. In this algorithm, the number of agents is divided into two subagents. Each subagent is assigned to focus solely on either exploration or exploitation. The comprehensive learning strategy generates exemplars for both subgroups. In the exploration sub-agent, exemplars are generated using the personal best experiences of agents within that same exploration space. The exploitation subagent generates the exemplars using the personal best experiences of all agents. This separation preserves exploration diversity even if exploitation converges prematurely. The algorithm is applied to optimize parameters of the 250 W and 500 W PEMFC models under varying conditions. Simulation results demonstrate the outperformance of the HCLBES algorithm in terms of convergence speed, estimation accuracy, and robustness compared to recent optimization algorithms. The effectiveness of HCLBES was also verified through statistical metrics and different commercial PEMFC models, including BCS 500 W stacks, Horizon 500, and NedStack PS6. Experimental validation confirms that the proposed algorithm effectively captures the nonlinear behaviours of PEMFCs under dynamic operating conditions. This research aligns with the Sustainable Development Goals (SDGs) by promoting clean and affordable energy (SDG 7) through the enhanced efficiency and reliability of PEMFCs, thereby supporting sustainable industrialization and innovation (SDG 9).

Keywords: proton exchange membrane fuel cell; optimization algorithm; parameter estimation; bald eagle search; heterogeneous comprehensive learning; sustainable development

check for updates

Academic Editor: Vida Maliene

Received: 18 September 2025
Revised: 12 October 2025
Accepted: 28 October 2025
Published: 31 October 2025

Citation: Ali, A.K.; Hussain, A.N.; Al-Obaidi, M.A.; Al-Anssari, S. Upgrading Sustainability in Clean Energy: Optimization for Proton Exchange Membrane Fuel Cells Using Heterogeneous Comprehensive Learning Bald Eagle Search Algorithm. *Sustainability* **2025**, *17*, 9729. https://doi.org/10.3390/su17219729

Copyright: © 2025 by the authors. Licensee MDPI, Basel, Switzerland. This article is an open access article distributed under the terms and conditions of the Creative Commons Attribution (CC BY) license (https://creativecommons.org/licenses/by/4.0/).

1. Introduction

The increasing demand for reliable, clean, and sustainable energy sources has markedly expedited the creation and use of the deployment of advanced energy conversion technologies [1]. Regardless, growing concerns over air quality degradation, the volatility of natural gas and crude oil prices, and the accelerating impacts of global climate change have intensified the global shift towards sustainable energy alternatives [2]. Various sustainable energy resource solutions have been proposed to address the growing global demand for clean, efficient, and environmentally responsible energy systems [3–5]. Among these, fuel cells, particularly proton exchange membrane fuel cells (PEMFCs), have developed as key technologies that contribute directly to sustainable development goals by promoting low-emission energy conversion, decreasing dependence on fossil fuels, and enhancing energy security in different power applications. However, the practical development and real-time control of PEMFC models is highly dependent on deriving accurate mathematical models that can replicate their complex, nonlinear, and dynamic behaviours under various operational conditions. Although there have been significant advancements in PEMFC research, challenges remain in the optimal design of fuel cell stacks that minimize material waste and extend system longevity, all of which are critical aspects of sustainability. A critical aspect of this endeavor is the development of accurate electrochemical models, which serve as foundational tools for performance analysis, controller design, and fault diagnosis [4–7]. Moreover, scalability and real-time adaptability remain key challenges for practical implementation in dynamic energy environments. Broader energy systems research, such as the work of [8], has also reported similar challenges regarding coordination, scalability, and optimization efficiency. Over the past few decades, diverse electrochemical modelling approaches have been proposed, differing in complexity and typically categorizing them into two broad classes: mechanistic (physics-based) models and semi-empirical models [9]. Mechanistic models use extensive electrochemical, thermodynamic, and transport equations to accurately represent the physical processes occurring inside the fuel cell. Semi-empirical models establish a balance between computational efficiency and the accuracy of physical representation, enabling precise estimates of nonlinear polarization behaviors and supporting real-time control strategies [10]. Among these models, the Amphlett model has emerged as a widely accepted standard due to its practical accuracy and broad adoption in the literature [11,12]. In earlier PEMFC models, the calibration efforts of empirical and semi-empirical correlations using nonlinear least-squares fittings yielded useful but often locally optimal parameter sets [11]. As fuel cell designs and operating regimes grew more complex, these classical approaches struggled to escape local minima or demanded extensive manual tuning. Thus, an accurate parameter estimation for such models has become a benchmark problem in development PEMFC models [13]. To address the parameter estimation challenge for the PEMFC model, a wide array of optimization approaches based on nature-inspired metaheuristic algorithms have been proposed in recent years. These include particle swarm optimization (PSO) [14], genetic algorithms (GA) [15], simple-GA [16,17], artificial bee colony (ABC) [18], and artificial immune systems (AIS) [19] for estimating the best parameters of the PEMFC model. Among these algorithms, GA and PSO have demonstrated promising results in addressing multi-objective nonlinear optimization problems [20,21] but they still have premature convergence, which limits their global search capability in minimization problems.

The PEMFCs have become a strong choice for use in electrical vehicles, hybrid power systems, and renewable energy resources due to their efficiency, ability to work at different temperature levels, quick start, small size, and production of no emissions [14,22–30].

Other recent methods used for the same task are war strategy optimization (WSO) [25], differential evolution (DE) [31,32], harmony search optimization (HSO) [33], grasshop-

per optimization algorithm (GOA) [34], biogeography-based optimization (BBO) [35], teaching–learning-based optimization (TLBO) [36], the Archimedes optimization algorithm (AOA) [22], multi-verse Optimizer (MVO), shark smell optimization (SSO) and ant lion optimizer (ALO) in [26], atom search optimization (ASO) [37], Cuckoo Search (CS) optimizer [38], salp swarm Algorithm (SSA) [39,40], flower pollination algorithm (FPA) [41], and whale optimization algorithm (WOA) [42].

Algorithms like the Harris hawks optimization (HHO) [43], bald eagle search (BES) optimizer algorithm [44], bird mating optimizer (BMO) [45], grey wolf optimizer(GWO) [46], and shuffled frog-leaping algorithm (SFLA) [13] have demonstrated varying degrees of accomplishment in exploring multimodal error landscapes without gradient information. Some swarm-based or bio-inspired algorithms also require fewer computational steps to reach near-optimal solutions compared to traditional optimization methods [37]. Numerous hybrid optimization techniques have been proposed due to their ability to balance exploration and exploitation in complex search spaces. These comprise the hybrid artificial bee colony (HABC) algorithm [23], hybrid vortex search algorithm [47], the heterogeneous comprehensive learning-based Archimedes optimization algorithm (HCL-AOA) which uses a heterogeneous comprehensive learning mechanism to enhance exploration and exploitation of the search algorithm [22], the JAYA algorithm with Nelder-Mead simplex refinement [30], and neural network-based swarm-optimization algorithms [48,49]. Among these, AOA enhanced through the comprehensive learning has demonstrated superior convergence performance and robustness across different PEMFC models. Comprehensive surveys on algorithmic approaches to PEMFC parameter identification are available in [2,50]. However, researchers are still working on creating optimization algorithms that can improve how quickly they find solutions in different fuel cell situations and can be trusted for real-time parameter extraction in PEMFC modular [51].

Literature Survey

Empirical and semi-empirical mathematical models of PEMFC originated from pioneering studies that established fundamental voltage–current correlations [11,12,52–54]. Amphlett et al. [11] developed an empirical model for the Ballard Mark IV cell, fitting activation and concentration overpotentials to polarization data via nonlinear regression and demonstrating accurate predictions over a limited current range [53]. Amphlett and colleagues explored scale-up effects in a PEMFC stack with a power rating of 5 kW, underscoring challenges in scaling parameters between models of fuel cells with different power ratings [52]. Rowe and Li [54] enhanced physics-based modeling by incorporating proton transport resistance and water management effects, improving dynamic performance predictions but highlighting sensitivity to initial parameter estimates of the PMFC model. Squadrito et al. [12] proposed streamlined expressions for activation and ohmic losses, offering simplified curve-fit parameters still used as benchmarks in later studies.

Nature-inspired metaheuristic optimization algorithms have widely addressed the limitations of local minima and manual tuning inherent in curve-fitting by accurately estimating parameters of mathematical models. Algorithms such as GA, PSO, and GWO, among other swarm-based techniques, have demonstrated strong potential for parameter estimation across several studies [14–17,19,22–28]. Meanwhile, adsvanced adaptive metaheuristics, including the HHO and the SSA, have further emphasized the critical balance between exploration and exploitation within the search space [28,30]. Such balance is essential to prevent premature convergence while maintaining search efficiency. Furthermore, swarm-based optimizers such as GA [15] and GWO [28,30], as well as physics-inspired methods like the ASO algorithm [24], highlight the value of dynamic learning mechanisms for enhancing the compactional robustness of algorithms and adaptability. Despite these

advances, online parameter identification frameworks for PEMFCs continue to face challenges related to real-time computational constraints [10]. These contrasting perspectives highlight the necessity for an optimization framework that minimizes user-dependent tuning parameters, enhances global search capability, and dynamically adapts to the nonlinear and multi-dimensional PEMFC error surface in real time. Kandidayeni et al. [13] benchmarked several metaheuristics on PEMFC modeling, concluding that no single method outperformed others universally, emphasizing the need for context-specific algorithms. Priya et al. [14] applied a standard GA to explore the PEMFC parameters, obtaining a better global solution as compared with gradient-based methods. However, the standard GA suffered from premature convergence due to insufficient mutation diversity. In addition, non-iterative resistance-based models and adaptive RNA GA techniques have also been used for the identification of model parameters, as reported in [6,15], respectively. While these approaches offer computational simplicity, they often suffer from convergence limitations or sensitivity to initial conditions.

Numerous studies have proposed variants of classical search algorithms to improve the accuracy of PEMFC modeling parameter estimation. For instance, Zhang et al. [23] introduced the HABC algorithm for PEMFC modeling, achieving faster convergence compared to traditional methods, though it remained susceptible to premature convergence. Similarly, Fathy and Rezk [24] applied MVO, showcasing promising estimation accuracy but encountering challenges in maintaining a balance between exploration and exploitation. Ayyarao et al. [25] introduced the WSO for accurate PEMFC parameter estimation, a militaristic-inspired approach incorporating dynamic update rules, which exhibited strong performance in high-dimensional search spaces.

In the same context, Alsattar et al. [55] presented the BES meta-heuristic algorithm, structuring search into surveying, swooping, swooping, and capturing phases to balance exploration and exploitation; however, its application to PEMFC parameter estimation remains unexplored across different fuel cell configurations. Rao et al. [26] employed the SSO optimizer, emphasizing its simplicity and global search capability, although its convergence rate diminished for higher-dimensional problems. Other studies have explored the probabilistic and physics-inspired algorithms. Abdel-Basset et al. [27] proposed a HBO algorithm, which integrates efficient data structures to accelerate the search process. Li et al. [28] introduced the SMS algorithm, demonstrating enhanced population diversity and improved avoidance of local optima. Although there have been advances in search algorithms, purely population-based algorithms often require extensive parameter tuning and are prone to stagnation in local optima. To overcome these issues, hybrid algorithms have been developed to leverage the complementary strengths of different metaheuristics. Fathy et al. [47] introduced an optimizer called Vortex Search with Differential Evolution (VS-DE) optimizer, which integrates Lévy-flight sampling into DE's mutation process to enhance convergence performance under varying operating conditions. Niu et al. [35] enhanced the BBO optimizer with mutation strategies (BBO-M) for efficient parameter identification in modeling the solar cells and PEMFCs. The algorithm improves the standard BBO algorithm by integrating mutation mechanisms inspired by DE and chaos theory to strengthen global search performance. The algorithm improves both the searching ability and the speed of convergence. Turgut and Çoban [36], proposed an enhanced TLBO with an elite retention approach to preserve high-quality solutions between iterations to speed convergence at the cost of added algorithm complexity. This modification accelerates convergence in parameter estimations in PEMFC modeling but introduces additional implementation complexity. Xu et al. [30] combined the JAYA algorithm with Nelder-Mead simplex refinement, employing JAYA for global exploration and simplex for local fine-tuning, which resulted in less error in fitting curves. It appears that these studies reveal the

development of numerous metaheuristic algorithms for PEMFC parameter identification. While effective to some extent, these methods often suffer from issues like premature convergence, limited exploration ability, and sensitivity to parameter tuning. A critical step in achieving the best performance and reliability of PEMFC models is the development of accurate mathematical models. Thus, the accuracy of such models is heavily dependent on accurate parameter estimation, which remains a challenging optimization task given the nonlinear, multivariable, and highly coupled nature of PEMFC dynamics. In order to address these challenges, this study proposes a novel optimization algorithm called the Heterogeneous Comprehensive Learning Bald Eagle Search (HCLBES) for accurate parameter estimation of different PEMFC models. The HCLBES algorithm improves the original Bald Eagle Search (BES) method by adding different learning strategies and a way to share memory more effectively. We carried out extensive tests using PEMFC models with two different power levels to evaluate the performance of an HCLBES algorithm. These include a PEMFC 250 W stack [30] and three widely used PEMFC 500 W stacks (NedStack PS6, BCS 500 W, and Horizon 500 W) [28]. The diverse characteristics of these fuel cell stacks provided a robust testbed for validating the adaptability and accuracy of the proposed algorithm. The primary contributions of this work can be summarized as follows:

- A novel optimization framework (HCLBES) is introduced, leveraging heterogeneous learning and comprehensive learning strategies to enhance search capabilities.
- The proposed HCLBES is applied for accurate parameter estimation of the different PEMFC model, which serves as a benchmark in the literature.
- Comparative analysis with state-of-the-art algorithms is presented to demonstrate the novelty of the proposed HCLBES superiority in terms of accuracy, convergence speed, and computational efficiency.
- Validation is carried out across multiple PEMFC stack ratings to confirm the robustness and versatility of the proposed method.

Based on the detailed review of search optimization methods, it appears that search optimization techniques are the best and most dependable way to determine the unknown parameters of PEMFCs. The literature uses various search algorithms to calculate the unknown parameters of the PEMFC stacks, as summarized in Table 1. These studies emphasize the necessity for a flexible, simple search optimizer technique that can effectively explore the solution space broadly and converge to optimal solutions rapidly, which was the motivation for the development of the novel HCLBES algorithm reported in this work.

To accurately determine the unknown parameters in the context of optimization challenges, it is essential to define the objective function, as it guides the algorithm to reach the optimal parameter values. In the literature, numerous studies used the sum of the squared errors (SSE) [14,15,23–30,47] as an objective function, while few have utilized the Mean Squared Error (MSE) [22]. Accordingly, in this study, the MSE is selected because it normalizes the error by the number of data points, providing a scale-independent measure that facilitates comparison across datasets of varying sizes. Furthermore, MSE fines larger errors more heavily due to the squaring operation, which can enhance optimization stability and lead to more accurate parameter estimation during the training process [22]. The rest of this paper is structured as follows: the proposed HCLBES algorithm is explained along with its implementation phases for application to PEMFC modules in Sections 2–4. Section 5 describes the formulation of the PEMFC model problem and the objective function. Section 6 features simulation and results. Section 7 presents a summarization of the results discussion. Finally, conclusions and outcomes are presented in Section 8.

Table 1. Comparison analysis of existing studies on various optimization algorithms for parameter estimation of diverse PEMFCs.

Ref.	Algorithm	Studied Fuel Cell-Model	Comparison Study				Objective Function	It	Np
			Modular–1	Modular–2	Modular–3	Modular–4			
[15]	ARNA-GA	Modular 1: PEMFC 250 W	SGA, HGA, Real-GA [17]	†	†	†	SSE	1000	50
[23]	HABC	Modular 2: PEMFC stack	Real-GA, H-GA, S-GA [23]	†	†	†	SSE	2000	–
[14]	S-GA	Modular 3: PEM 250 W	BIPOA, PSO, SGA, HGA [14], Real-GA [17], AIS [19]	†	†	†	SSE	100–500	20–30
[24]	MVO	Modular 1: PEMFC 250 W	HGA, SGA [16], HADE [32], Real-GA [17], and HABC [23]	†	†	†	SSE	2000	50
[26]	Shark Smell	Modular 1: PEMFC250 W	TLBO-DE [45], ARNA-GA [23], Real-GA, MPSO, and QPSO [26], Sa-DE, HIS, and STLBO [56]	†	†	†	SSE	500	100
[30]	JAYA	Modular 1: PEMFC 250 W	GOA, GWO, SSO, MVO, JAYA, and, JAYA−NM [30]	†	†	†	SSE	5000	30
[28]	SMS	Modular 1: BCS 500 W Modular 2: NedStackPS6 Modular 3: Harizon500 W Modular 4: PEMFCs250 W	FOA, SFLA, and ICA [49], VSA [47], SSO [26], NNA [24], VSDE, SP-UCI, and ISCE [28], DEM, GWO, SSO [40]	SP−UCI, SCE−UA, ISCE [28], VSDE, VSA [47], NNA [45], FOA, ICA [13], SSO [40], GA, GHO [34]	SP−UCI, SCE−UA, and ISCE [28], SFLA [13]	SP−UCI, SCE−UA, and ISCE [28], JAYA−NM, MVO, GWO, JAYA [30]	SSE	5000	–
[47]	VSDE	Modular 1: BCS 500 W Modular 2: NedStackPS6 Modular 3: SR-12 PEM 500 W Modular 4: PEMFCs250 W	SSO [40], SSO [26]	GHO [34] SSO [40]	GWO [47], SSO [26]	STLBO, and TLBO [56], ITHS [57], HABC [23], MVO [24], Real GA [17]	SSE	500	50
[27]	IHBO	Modular 1: BCS 500 W Modular 2: NedStackPS6 Modular 3: H-12 stack Modular 4: SR-12 500 W	WOA [42], FPA [41], HBO, ISA, MFO, MRFO, EO, AEO, TSA, and STSA [27], SSA [40]	WOA [42], FPA [41], HBO, ISA, MFO, MRFO, EO, AEO, TSA, and STSA [27], SSA [40]	WOA [42], FPA [41], HBO, ISA. MFO, MRFO, EO, AEO, TSA, and STSA [27], SSA [40]	WOA [42], FPA [41], HBO, ISA, MFO, MRFO, EO, AEO, TSA, STSA [27], SSA [40]	SSE	5000	–
[22]	HLCAOA	Modular 1: BCS500 W Modular 2: NedStackPS6 Modular 3: SR-12 500 W Modular 4: PEMFC 250 W	VSDE, VSA [47]	VSDE, VSA [47]	VSDE, VSA [47]	VSDE, VSA, and ABC[47], MVO [22], HABC [24], ITHS [57], STLBO.TLBO [56], Real-GA [17]	MSE	2000	100
[29]	BES	Modular1: Avista SR-12	ALO, BES, COOT, EO, HBO [29]	†	†	†	SSE	–	–
[25]	WSO	Modular 1: BCS500 W Modular 2: NedStackPS6 Modular 3: Harizon250 W Modular 4: Horizon500 W	SFLA, FOA, and ICA [13], NNA [25], HHO [43], GWO [46], Shark-Smell [26]	BES [44], IBHO [27], AEFA, IAEO, STSA, NNA, and EO [13], SFLA, FOA, and ICA [13], SSO [40], GOA [34], VSDE and VSA [47]	†	ISCE [42], GWO [46], SFLA [13], HHO [43]	SSE	1000	50

"†" indicates that the PEMFC modular was not considered in this study, "–" refers to the not-specified value of the parameter in reference. It represents the maximum number of iterations used, and Np search size.

2. Mathematical Model of PEMFC

The electrochemical model of fuel cells (FCs) is widely used in modeling and simulation studies because it effectively represents the fundamental electrochemical processes governing FC operation, as explained in detail in [11,28,53]. Among these models, the model proposed by Squadrito et al. [53] is considered the most suitable and practical, as it requires only voltage and current measurements, thereby minimizing sensor requirements. This model accurately simulates the physical behaviour of a cell by integrating an FC, which includes parameters with clear physical significance. However, it does not fully capture the mass transport phenomena that influence performance [10].

Figure 1 shows the schematic configuration of the PEMFC, which consists of a cathode, anode, and electrolyte. The FC system processes involved a hydrogen supply to the anode, where it is oxidized to produce protons and electrons. The protons pass through the electrolyte (proton exchange membrane), while the electrons flow through an external circuit to the cathode, generating electrical power. At the cathode, oxygen reacts with the incoming protons and electrons to form water as the only by-product.

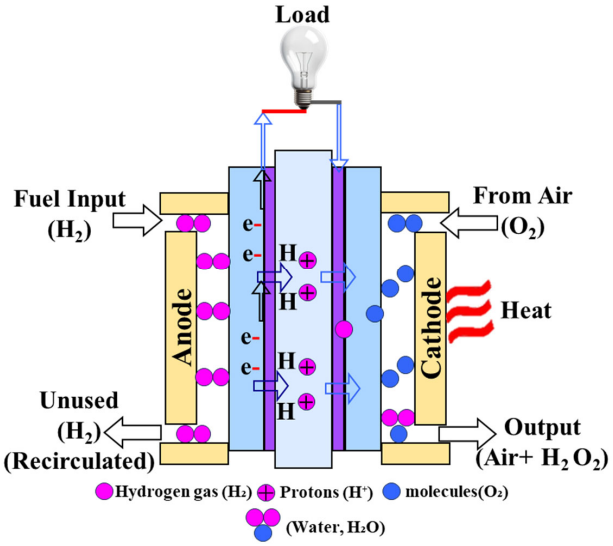


Figure 1. Simplified configuration of PEMFC.

The catalysts used in the FC system are employed to lower the activation energy required for hydrogen oxidation. During operation, electrons flow through an external circuit to generate an output voltage, while protons migrate through the electrolyte. The PEMFC primarily operates through the following electrochemical reactions occurring in a hydrogen–oxygen system [54].

Anode Reaction Oxidation: At the anode, hydrogen gas H_2 is oxidized by releasing protons H^+ and electrons e^-. A catalyst, often platinum, facilitates this process by separating hydrogen molecules efficiently into their constituent protons and electrons [28].

$$H_2 \rightarrow 2H^+ + 2e^- \quad (1)$$

$$2H^+ + 2e^- + \frac{1}{2}O_2 \rightarrow H_2O \quad (2)$$

Cathode ***Reaction Reduction:*** At the cathode, oxygen gas O_2 mixes with protons and electrons from the electrolyte, and the electrons travel through the external circuit. The reduction reaction generates water H_2O and heat [10]. Combining the anode and cathode reactions yields the overall chemical reaction, which can be expressed as follows:

$$H_2 + 2e^- + \frac{1}{2}O_2 \rightarrow \mathrm{H_2O} \tag{3}$$

The terminal voltage of a PEMFC can be defined as follows [14]

$$V_{FC} = E_{Nernst} - (V_{act} + V_{ohm} + V_{Con}) \tag{4}$$

V_{act} represents the activation voltage drop, V_{ohm} denotes the ohmic voltage drop, and V_{Con} corresponds to the concentration voltage drop. The term E_{Nernst} signifies the reversible thermodynamic potential and is defined as follows [47]:

$$E_{Nernst} = E_0 + \frac{RT_K}{\zeta F}\ln\left(P_{H_2}\sqrt{P_{O_2}}\right) \tag{5}$$

E_0 represents the reference voltage, F is Faraday's constant, R is the universal gas constant, and T_K is the cell temperature in Kelvin. Additionally, ζ represents the number of electrons transferred, while P_{H_2} and P_{O_2} represent the partial pressures of hydrogen and oxygen, respectively. An alternate expression of Equation (5) is provided as follows [47]

$$E_{Nernst} = 1.229 - 8.5 \times 10^{-4}(T_K - 298.15) + 4.385 \times 10^{-4} T_K \ln\left(P_{H_2}\sqrt{P_{O_2}}\right) \tag{6}$$

The activation voltage drop is mathematically expressed as:

$$V_{act} = \frac{RT_K}{2\alpha F}\ln\left(\frac{i}{i_0}\right) \tag{7}$$

i represents the fuel cell current, i_0 denotes the exchange current density, and α is the transfer coefficient. This expression can be reformulated as follows:

$$V_{act} = -(\eta_1 + T_K(\eta_2 + \eta_3 \ln(C_{O_2}) + \eta_4 \ln(i))) \tag{8}$$

η_1, η_2, η_3, and η_4 are empirical coefficients, i is the fuel cell current, and C_{O_2} represents the oxygen concentration, which is defined as:

$$C_{O_2} = \frac{P_{O_2}}{5.08 \times 10^6} exp\left(-\frac{498}{T_K}\right) \tag{9}$$

The ohmic voltage drop within the fuel cell arises due to its internal resistance and is defined as:

$$V_{ohm} = i\left(\frac{\mathrm{r}_M \ell}{A} + R_c\right) \tag{10}$$

The membrane resistivity is given by:

$$\mathrm{r}_M = \frac{181.6\left[1+3\times10^{-3}\left(\frac{i}{A}\right)+62\times10^{-3}\left(\frac{T_K}{303}\right)\left(\frac{i}{A}\right)^{2.5}\right]}{\left[\lambda-0.634-3\left(\frac{i}{A}\right)\right]*\exp\left(4.18\left(\frac{T_K-303}{T_K}\right)\right)} \tag{11}$$

r_M represents the membrane resistivity, ℓ is the membrane thickness, A denotes the active cell area, and λ refers to the membrane water content. The concentration voltage drop is calculated as follows:

$$V_{Con} = -b\ln\left(1 - \frac{i}{i_{max}A}\right) \tag{12}$$

b is a constant and i_{max} represents the maximum current density. Thus, the overall voltage of a PEMFC stack with n_s series-connected cells can be calculated using the following formula:

$$V_{Stack} = n_s(E_{Nernst} - V_{act} - E_{ohm} - V_{Con}) \tag{13}$$

The parameters under evaluation include η_1, η_2, η_3, η_4, λ, R_c (contact resistance to electron conduction), and b [22].

These parameters directly influence the predicted cell voltage: overpotential coefficients $\eta_1 - \eta_4$ affect the activation losses, λ affects proton conductivity and overall membrane performance, R_c regulates resistive losses in electron conduction, and b controls the slope of the voltage–current relationship. Understanding the sensitivity of cell voltage to these parameters is essential for accurate modeling and optimization of PEMFC performance.

3. Bald Eagle Search (BES) Optimization Algorithm

The BES algorithm is a meta-heuristic optimization algorithm inspired by the hunting behaviours of bald eagles [55]. It is particularly well-suited for PEMFC parameter identification because it efficiently handles high-dimensional and nonlinear search spaces, which are common in electrochemical modeling [10]. The BES structured exploration and exploitation phases allow it to avoid local minima while rapidly converging to the global optimum. This capability is crucial when estimating multiple interdependent parameters, such as activation overpotentials, membrane water content, and resistances, ensuring accurate voltage prediction and robust model performance. The BES consists of three main stages:

1. **Selection stage (defining the search space):** The eagle selects an appropriate search space based on its prior movements, as expressed by:

$$Z_{i,t+1} = Z_{best_i} + \xi \times r_i(Z_{mean_i} + Z_{i,t}) \tag{14}$$

$Z_{i,t+1}$ represents the updated position after the selection stage, Z_{best_i} optimal search position, ξ location update parameter ($1.5 \leq \xi \leq 2$), r_i random coefficient [0 to 1], Z_{mean_i} mean position from the previous search, and $Z_{i,t}$ is the current position of the eagle in the search space at iteration t.

2. **Search stage (Spiral Flight to Explore the Space):** It explores the space using a spiral flight pattern to locate the best dive position.

$$\begin{gathered} Z_{i,t+1} = Z_{(i,t)} + Y_{(i,t)} \times (Z_{(i,t)} - Z_{(i,t+1)}) + X_{(i,t)} \times (Z_{(i,t)} - Z_{mean_i}) \\ X_{(i,t)} = \frac{X_{r(i,t)}}{\max(\lceil X_r \rceil)},\ Y_{(i,t)} = \frac{Y_{r(i,t)}}{\max(\lceil Y_r \rceil)} \\ X_{r(i,t)} = r_{(i,t)} \times \sin\left[\theta_{(i,t)}\right],\ Y_{r(i,t)} = r_{(i,t)} \times \cos\left[\theta_{(i,t)}\right] \\ \theta_{(i,t)} = \mathrm{A} \times \pi \times r,\ r_{(i,t)} = \theta_{(i,t)} + R \times r \end{gathered} \tag{15}$$

$X_{(i,t)}$, and $Y_{(i,t)}$ are directional coordinates between 0 and 1 for determining the updated position with respect to the polar axis, respectively, $X_{r(i,t)}$, and $Y_{r(i,t)}$ represent intermediate values that determine how much the eagle moves in a spiral pattern, A is a constant parameter (5 to 10), R is the search period control that takes values between 0.2 and 2, while $r_{(i,t)}$, and $\theta_{(i,t)}$ are polar diameter and angle in spiral motion in polar coordinates, respectively [29].

3. **Swooping stage (Diving Toward the Optimal Solution):** The eagle executes a final descent toward the prey while others in the population also move toward the optimal position:

$$\begin{gathered} Z_{i,t+1} = Rand \times Z_{best_i} + \mathrm{X}_1(i,t) \times (Z_{(i,t)} \times \mathrm{C}_1 \times Z_{mean_i}) + \mathrm{Y}_1(i,t) \times (Z_{(i,t)} \times \mathrm{C}_2 \times Z_{best_i}) \\ \mathrm{X}_1(i,t) = \frac{\mathrm{Y_r}(i,t)}{\max(\lceil \mathrm{X}_r \rceil)},\ \mathrm{Y}_1(i,t) = \frac{\mathrm{Y_r}(i,t)}{\max(\lceil \mathrm{Y}_r \rceil)} \\ \mathrm{X_r}(i,t) = r_{(i,t)} \times \sinh\left[\theta_{(i,t)}\right],\ \mathrm{Y_r}(i,t) = r_{(i,t)} \times \cosh\left[\theta_{(i,t)}\right] \\ \theta_{(i,t)} = \mathrm{A} \times \pi \times r,\ r_{(i,t)} = \theta_{(i,t)} \end{gathered} \tag{16}$$

C_1 and C_2 represent movement velocities (1 to 2).

4. The Proposed HCLBES Optimization Algorithm

This section presents the novel Heterogeneous Comprehensive Learning-Based Bald Eagle Search (HCLBES) algorithm, developed to improve the efficiency of parameter estimation in PEMFC fuel cells. The first subsection describes the Comprehensive Learning (CL) strategy, which preserves agent diversity and effectively balances exploration and exploitation. It is followed by clarification of the heterogeneous Comprehensive Learning (HCL) integration with the BES to develop an advanced search optimization algorithm.

4.1. Heterogeneous Comprehensive Learning

The CL approach is a strategy that enables search agents to exchange information and experiences, ensuring an optimal balance between exploration and exploitation. In order to prevent premature convergence, agent diversity must be preserved across multiple dimensions, achieved by leveraging each agent's most effective past experiences, termed exemplars. In CL, the exemplar for each dimension is selected based on a probabilistic learning function, where the probability of choosing a given dimension follows [58].

$$P_{Cl_i} = q_1 + q_2 \frac{\exp\left(\frac{10(i-1)}{(p_s-1)}\right) - 1}{(\exp(10) - 1)},\ i = 1, 2, \ldots, N \tag{17}$$

where N represents the number of search agents, q_1 and q_2 are constants with values 0.05 and 0.22, respectively, and p_s is constant [58]. The selection process for exemplars follows a probabilistic decision rule: if a randomly generated number exceeds P_{Cl_i}, the agent learns from its own prior experience; otherwise, it adopts knowledge from another agent selected based on its outcome of fitness function value.

Algorithm 1 describes the steps for determining exemplars related to the CL technique, where a random number is compared to given agent probability state P_{Cl_i}, for each dimension d of the i-th agent.

Algorithm 1. Steps of Comprehensive Learning Strategy.

1. **Initializations:** The process starts by setting the dimension counter ($d = 1$).
2. **Probabilistic Decision:** The process compares each individual state (P_{Cl_i}) to the random number r for each d.
3. **Exploratory Learning** (**Yes**): If $\{r < P_{Cl_i}\}$, two potential exemplar components are generated (${f1_i}^d = [{r_i}^d * N]$, ${f2_i}^d = [{r_i}^d * N]$), and the chosen one states that it has the best objective function ${f_i}^d$ value according to decision $\{Z_{best,{f1_i}^d} > Z_{best,{f2_i}^d}\}$.
4. **Individual Learning** (**No**): the objective value is simply set to the agent index (i) ${f_{i-1}}^d = {f_i}^d$.
5. **Iteration:** $d = d + 1$, and the process repeats until all dimensions (D_{max}) are covered.
6. **Termination:** The strategy ends after processing all dimensions.

Proof of Algorithm 1: with $D_{max} = 2$

Given: Number of agents $N = 3$, $q_1 = 0.05$, $q_2 = 0.22$, $p_s = 2$,

Random numbers $r_{N,D} = \begin{bmatrix} 0.12 & 0.3 \\ 0.05 & 0.18 \\ 0.25 & 0.10 \end{bmatrix}$

Step 1: Compute probabilities P_{Cl_i} for each agent $i = 1, 2, 3$:

Agent 1: $P_{Cl_1} \approx 0.05$
Agent 2: $P_{Cl_2} \approx 0.27$
Agent 3: $P_{Cl_3} \approx 0.49$
Step 2: Select Exemplars for each dimension ($d = 1, 2$).
Agent 1, Dimension 1: $r = 0.12 > P_{Cl_1} = 0.05 \rightarrow true \rightarrow$ *learns from another agent.*
Agent 1, Dimension 2: $r = 0.30 > P_{Cl_1} = 0.05 \rightarrow true \rightarrow$ *learns from another agent.*
Agent 2, Dimension 1: $r = 0.05 < P_{Cl_2} = 0.27 \rightarrow true \rightarrow$ *selects own past experience.*
Agent 2, Dimension 2: $r = 0.18 < P_{Cl_2} = 0.27 \rightarrow true \rightarrow$ *selects own past experience.*
Agent 3, Dimension 1: $r = 0.25 < P_{Cl_3} = 0.49 \rightarrow true \rightarrow$ *selects own past experience.*
Agent 3, Dimension 2: $r = 0.10 < P_{Cl_3} = 0.49 \rightarrow true \rightarrow$ *selects own past experience.*
Step 3: Update agent positions.

Using the selected exemplars for each dimension, agents update their positions according to the CL strategy Equations (19)–(21). This ensures diversity is preserved across all dimensions, preventing premature convergence while enabling adequate exploration and exploitation. □

4.2. Heterogeneous Comprehensive Learning Bald Eagle Search (HCLBES) Algorithm

To improve the performance of the BES algorithm in solving nonlinear and multidimensions optimization problems, the HCLBES modifies the agent movement strategy by categorizing the population into two heterogeneous subgroups. The first subgroup is responsible for diversification and engages in global exploration, while the second subgroup emphasizes intensification and refines promising solutions through local exploitation.

Diversification Subgroup (Exploration Phase): In the diversification phase, agents explore the search space based on an updated position equation that integrates exemplars determined via CL. This phase also includes an acceleration coefficient τ, which is subject to sigmoid function to regulate exploration intensity:

$$\tau(t) = \tau_{Max} + \frac{(\tau_{min} - \tau_{max})}{1 + \exp(-10(\frac{2t}{t_{max}} - 1))} \tag{18}$$

$\tau_{min} = 1.5$, $\tau_{max} = 3$, and t_{max} represents the maximum number of iterations.
The updated position of each search agent in this phase follows:

$$Z_{i,t+1} = Z_{i,t} + \tau(t).r.(Z_{best,t} - Z_{i,t}) + \tau(t).\text{Rand}.(exemplar_{i,t} - Z_{i,t}) \tag{19}$$

$Z_{i,t}$ is the position of agent i at iteration t, and $Z_{best,t}$ is the current best solution.

Intensification Subgroup (Exploitation Phase): In this phase, agents improve solutions by studying both the global best solution and the example created by CL. This prevents them from becoming stuck in local optima. In this phase, the position update takes the following form:

$$Z_{i,t+1} = \begin{cases} Rand \times Z_{best_i} + \mathrm{X}_1(i,t) \times \tau_1(t) \times \left(exemplar_{i,t} \times \mathrm{C}_1 \times Z_{mean_i}\right) + & p_s \geq 0.5 \\ \mathrm{Y}_1(i,t) \times \tau_1(t) \times \left(exemplar_{i,t} \times \mathrm{C}_2 \times Z_{best_i}\right) & \\ Rand \times Z_{best_i} + \mathrm{X}_1(i,t) \times \tau_2(t) \times \left(exemplar_{i,t} \times \mathrm{C}_1 \times Z_{mean_i}\right) + & p_s < 0.5 \\ +\mathrm{Y}_1(i,t) \times \tau_2(t) \times \left(exemplar_{i,t} \times \mathrm{C}_2 \times Z_{best_i}\right) & \end{cases} \tag{20}$$

$\tau_1(t)$ and $\tau_2(t)$ are dynamic acceleration coefficients that adjust linearly over iteration to maintain diversity and enhance exploitation efficiency. Furthermore, the p_s denotes a random probability uniformly distributed between 0 and 1, which determines whether an agent follows the exploration ($p_s \geq 0.5$) or exploitation ($p_s < 0.5$) behaviour during

position updates. This probabilistic switching maintains balance between subgroup actions and helps prevent premature convergence [58].

$$\tau_1(t) = 2.5 - \frac{2t}{t_{max}},\ \tau_2(t) = 0.5 + \frac{2t}{t_{max}} \tag{21}$$

The variable g_1 represents the number of search agents assigned to the diversification subgroup, while g_2 denotes the number of agents in the intensification subgroup. The sizes of both subgroups are determined as fixed proportions of the population size (typically $g_1 = \frac{N}{2}$, $g_2 = \frac{N}{2}$), following standard heterogeneous population strategies to balance exploration and exploitation [22].

The $exemplar_{i,t}$ represents the specific exemplar determined for the ith agent during t iteration, according to the CL strategy outlined in Algorithm 1. The optimal solution derived through the proposed HCLBES is visually represented in Algorithm 2, while the corresponding best solution is shown in the flowchart in Figure 2.

Algorithm 2. Pseudo code of the HCLBES.

1. Determine the values of the HCLBES parameters (population size N, maximum iterations t_{max}, learning coefficients C_1, C_2, C_3, and C_4, and subgroup sizes g_1 and g_2).
2. Initialize population Z with N solutions of dimension D_{max} using Equation (14).
3. Divide the population Z into two subgroups: g_1 and g_2.
4. Initialize the local best p_{best}, global best g_{best}, and velocities for each subgroup using Equation (20).
5. Evaluate the fitness of each individual in Z and identify best solutions: Z_{best}, p_{best}, and g_{best}.
6. Use CL-concept to set initial exemplars for g_1 and g_2 using Algorithm 1.
7. Compute acceleration coefficients τ, τ_1 and τ_2 using Equations (18) and (21).
8. Set iteration counter $t = 1$.
9. While $t \leq t_{max}$ do:
10. Update the velocities Z_v using Equation (20).
11. Update the parameters τ and d using Equations (18) and (19).
12. {Diversification for subgroup g_1}
13. Update the positions of population in g_1 using Equation (20).
14. Update p_{best} and g_{best} if improved.
15. {Intensification for subgroup g_2}
16. Update the positions of population in g_2 using Equation (20).
17. Update p_{best} and g_{best} if improved. {objective Evaluation}
18. Evaluate the new objective values of the entire population Z
19. Update the best solution, referred to as Z_{best}, along with the corresponding best personal and global solutions.
20. {Exemplar Update for g_1}
21. for each agent $i = 1$ to size(g_1) do
22. Generate a random number r.
23. Compute learning probability P_{Cl_i} using Equation (17).
24. Select two random indexes ${f_1}^d$, ${f_2}^d$ for $d = 1, \ldots, D_{max}$.
25. if $r > P_{Cl_i}$ then; if {objective $(Z_{f1_i{}^d})$ > objective $(Z_{f2_i{}^d})$} then; Set $Z_{\text{Exemplar(i)}} = Z_{f2_i{}^d}$
26. Else, Set $Z_{\text{Exemplar(i)}} = Z_{f1_i{}^d}$, end if
27. else

Algorithm 2. *Cont.*

28. Set $Z_{\text{Exemplar(i)}} = Z_{(i)}$, end if
29. end for
30. {Exemplar Update for g_2}
31. for each agent $i = 1$t o size(g_2) do
32. Generate a random number r.
33. Compute learning probability P_{Cl_i} using Equation (17).
34. Select two random indexes ${f1_i}^d$, ${f2_i}^d$ for $d = 1, \ldots, D_{max}$.
35. if $r > P_{Cl_i}$ then
36. if {objective $(Z_{{f1_i}^d})$ > objective $(Z_{{f2_i}^d})$} then Set $Z_{\text{Exemplar(i)}} = Z_{{f2_i}^d}$
37. Else, Set $Z_{\text{Exemplar(i)}} = Z_{{f1_i}^d}$, end if
38. Else: Set $Z_{\text{Exemplar(i)}} = Z_{(i)}$, end if
39. end for
40. Increment iteration counter: t = t + 1.
41. end while
42. Return the best solution, Z_{Best}

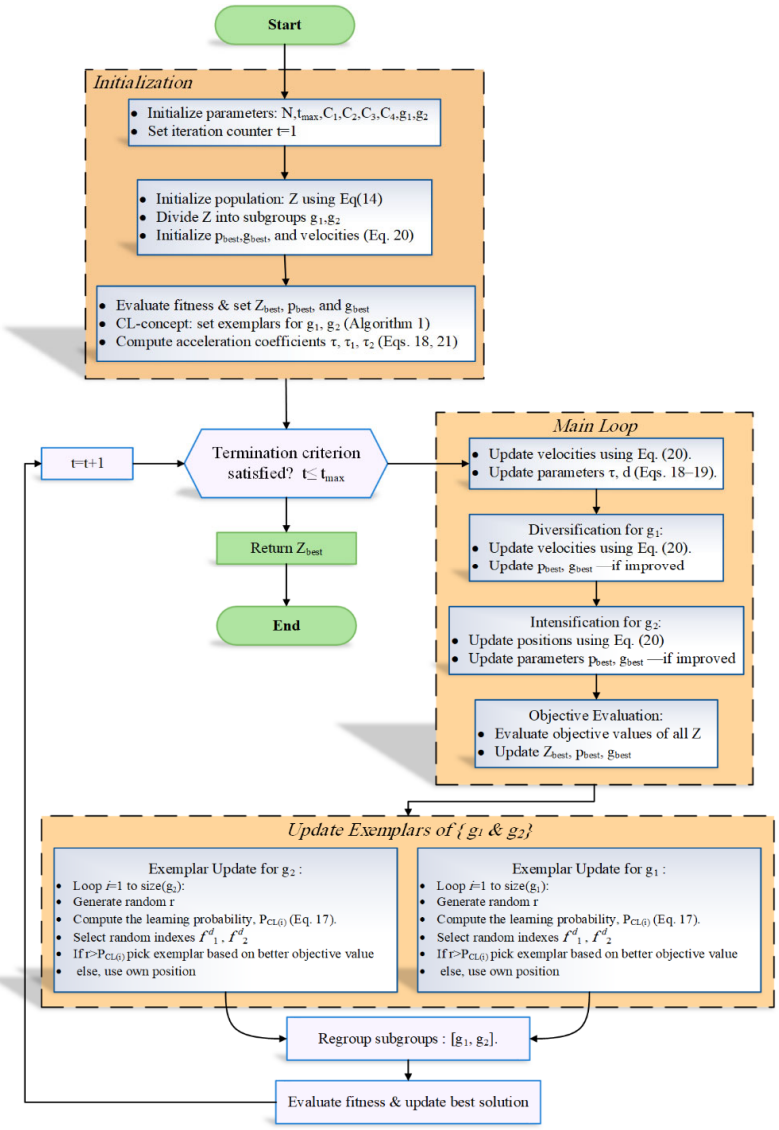


Figure 2. Flowchart of the HCLBES algorithm.

5. Formulation of the Optimization Model

The aim of this work is to refine PEMFC model parameters to closely replicate actual dynamic system behaviors and achieve high-fidelity simulation for sustainable energy applications. Due to the non-disclosure of certain important parameters by PEMFC manufacturers, the modelling method necessitates an assessment of their ideal values. The polarization curve on the manufacturer's datasheet for the fuel cell serves as a benchmark for this achievement, demonstrating empirical performance. The mathematical model of the PEMFC described in the previous section should be validated against experimental data to ensure its accuracy. The studied model of the PEMFC includes seven parameters (η_1, η_2, η_3, η_4, λ, R_c and b), each of which plays a critical role in determining the overall performance of the PEMFC stack.

The seven empirical parameters η_1, η_2, η_3, η_4, λ, R_c and b correspond to various factors: activation overpotential (intercept term), logarithmic current dependence, temperature correction in activation loss, partial pressure effects on activation overpotential, the number of water molecules per sulfonic acid group in the membrane, contact resistance, and the empirical coefficient in the concentration (mass transport) loss term. The coefficient η_1 is related to the voltage loss from base activation. Coefficient η_2 controls the rate at which voltage drops with current density. The η_3 adjusts the activation loss due to temperature effects, while η_4-related adjustments are based on the activation term influenced by gas pressure. Furthermore, the empirical coefficient λ related to membrane water content affects proton conductivity and water transport in the membrane group, and the electronic resistance coefficient R_c is related to the effective contact and electronic resistance between layers. Finally, the coefficient b governs the exponential decay of voltage at high current densities [11]. Accurate estimation of these parameters is crucial for reliable model predictions.

The objective function is essential for determining the unknown parameters of the PEMFC using experimental data. Thus, the validity of the developed model is evaluated by ensuring that the output voltage curves closely align with the experimental data, which is achieved by minimizing the MSE between the observed and simulated terminal voltages.

$$\text{Minimize } f_{MSE} = \frac{1}{n}\sum_{k=1}^{N}\left(V_{exp,k} - V_{est,k}\right)^2 \tag{22}$$

The MSE for PEMFC model is a quantitative measure that indicates the difference between the values predicted by PEMFC mathematical model and the corresponding experimental data, and it is defined as follows [22]:

$$f_{MSE} = \frac{1}{N_p}\sum_{x=1}^{N}\left(\frac{(V_{exp,}(x) - \gamma(T_k, RH_a, RH_c, P_a, P_c, i(j), A)}{-\beta(\eta_1, \eta_2, \eta_3, \eta_4, T_K, RH_c, P_c, i(j), A) - \varphi(T_K, i(j), A, \lambda, R_c) - \epsilon(i(j), b(T_k))}\right)^2 \tag{23}$$

The objective function includes variables such as the relative humidities of the cathode and anode vapors, RH_c and RH_a, respectively. P_a and P_c denote the inlet pressures at the anode and cathode, respectively, and N_p is the total number of data points. The parameters γ, β, φ and ϵ are nonlinear functions that encapsulate the voltage loss components [22]. The models are governed by a series of predetermined restrictions, formalized to guarantee physical feasibility and computational resilience. The PEMFC model is subjected to the constraints written as follows:

$$\begin{gathered} \eta_{Min,i} \le \eta_i \le \eta_{Max,i},\ i = 1,2,3,4 \\ \lambda_{Min} \le \lambda \le \lambda_{Max} \\ R_{c,Min} \le R_c \le R_{c,Max} \\ b_{Min} \le b \le b_{Max} \end{gathered} \tag{24}$$

The acceptable limits for the seven unknown parameters come from the technical details of different PEMFC stack designs, and the best limits are selected through careful simulation studies. The optimal parameter values are obtained when the objective function f_{MSE} attains its minimum while simultaneously meeting the feasible solutions within the parameter constraint limit. Figure 3 illustrates the process for parameter identification in the PEMFC model using the HCLBES algorithm.

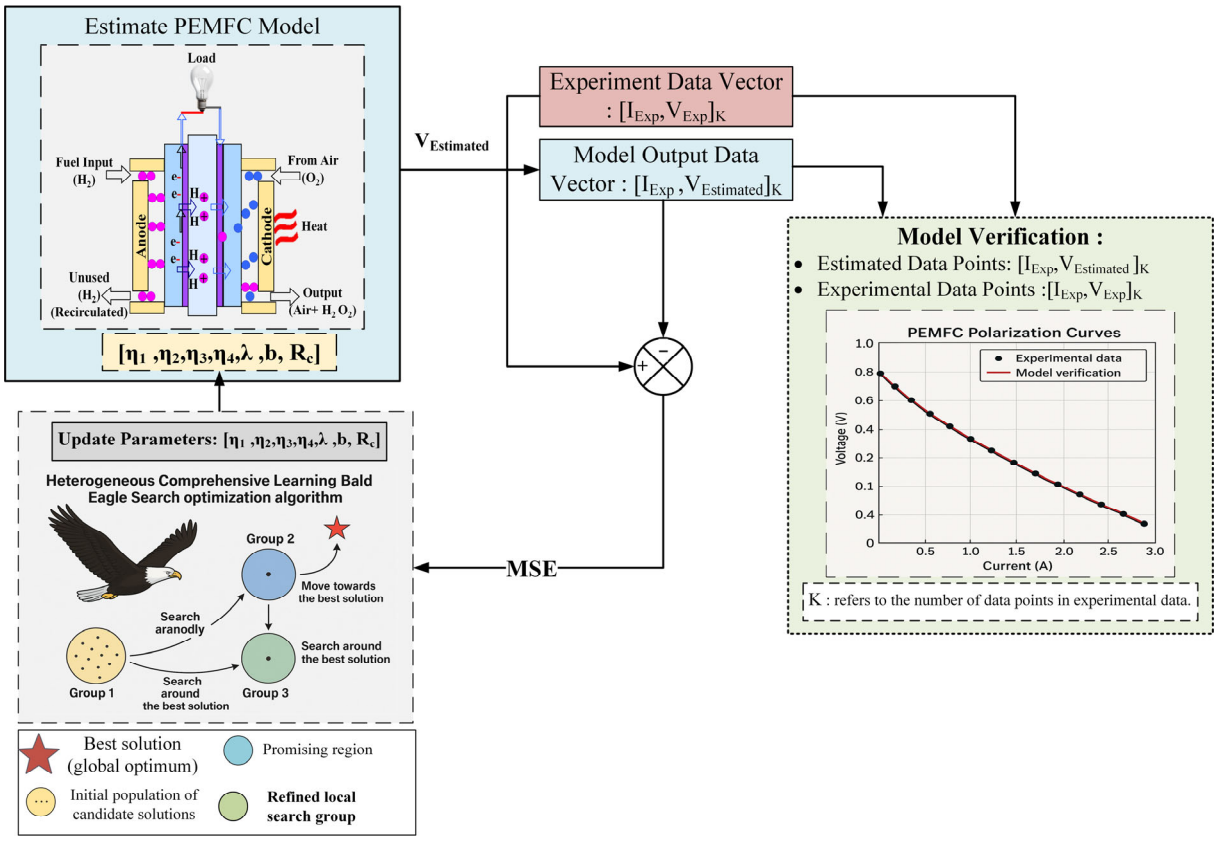


Figure 3. Schematic representation of the parameter estimation procedure for the PEMFC model using the HCLBES algorithm.

6. Simulation-Based Analysis and Results

The performance of the HCLBES is carefully assessed using the PEMFC model, which incorporates several sets of experimental data collected under different operating conditions. Two distinct power ratings for PEMFCs are investigated: 250 W and 500 W stacks, including models such as the NedStack PS6, BCS 500 W, and Horizon 250 W and Horizon 500 W [30]. In order to benchmark HCL−BES performance, several contemporary metaheuristic algorithms are employed for comparison, including the standard BES [44], HHO [43], ASO [37], GWO [46], and SSA [39]. All algorithms are implemented using native functions in MATLAB 2022b and executed on a computing platform equipped with an Intel Core i7-13700H processor (2.4 GHz) and 16 GB RAM. Each algorithm undergoes 30 independent trial runs, with each run consisting of 2000 iterations and a population of 100 agents. Table 2 summarizes the corresponding electrical specifications for these PEMFC models [22,28,46]

Table 2. Electrical Characteristics of the PEMFC models.

Parameters	PEMFC-250 W Stack-Model	PEMFC-500 W Stack-Model		
	Horizon 250 W	**Nedstack PS6**	**BCS 500 W**	**Horizon 500 W**
n_s	24	65	32	36
A(cm^2)	27	240	64	52
j_{Max} $(A.cm^2)$	0.86	1.4	0.469	0.025
l (µm)	127	178	178	0.51923
P_a(bar)	1.0–3.0	0.5–5	1	1
P_c (bar)	1.0–5.0	0.5–5	0.2075	0.55
T_k (k)	343.15–353.15	343	333	333
RH_a	1.0	1.0	1.0	1
RH_c	1.0	1.0	1.0	1

For modelling purposes, it is assumed that both the anode and cathode operate at 100% relative humidity, with the inlet pressure level in bars in accordance with prior literature [52]. As a prerequisite to the optimization process, the boundaries for the parameters to be estimated that majorly impact the searching ability of the algorithm are outlined in Table 3 [46].

Table 3. The employed upper and lower ranges of the PEMFC parameters.

Fuel Cell	Ranges		η_1	η_2	η_3	η_4	λ	R_c (Ω)	b (V)
250 W-stack	Range-1	Upper bound	−0.944	$5\,\varepsilon^{-3}$	$7.8\,\varepsilon^{-5}$	$-1.88\,\varepsilon^{-5}$	23	$8\,\varepsilon^{-4}$	0.5
		Lower bound	−0.952	$1\,\varepsilon^{-3}$	$7.4\,\varepsilon^{-5}$	$-1.98\,\varepsilon^{-5}$	14	$1\,\varepsilon^{-4}$	0.016
500 W-stack	Range-2	Upper bound	−0.8532	$33{,}487\,\varepsilon^{-3}$	$9.80\,\varepsilon^{-5}$	$-9.54\,\varepsilon^{-5}$	23	$8\,\varepsilon^{-4}$	0.5
		Lower bound	−1.19969	$33{,}487\,\varepsilon^{-3}$	$3.60\,\varepsilon^{-5}$	$-26\,\varepsilon^{-4}$	13	$1\,\varepsilon^{-4}$	0.0136

Scientific notation ε^n refers to 1×10^n, where n is a real integer value.

6.1. Parameter Identification for PEMFC 250 W Stack-Models

In this subsection, two experimental datasets obtained from a 250 W PEMFC stack are utilized to estimate seven unknown parameters of the model. Parameter estimation is performed over two distinct ranges, as detailed in Table 3. The seven unknown parameters of the equivalent circuit model are estimated using two sets of data that represent operating conditions of 1/1-bar at 343.15 K, and 3/5 bar at −353.15 K (pressures and temperature of anode and cathode). The parameter estimation was performed using the proposed HCLBES, along with the BES and other benchmark algorithms. Table 4 shows a comparison of seven parameters identified, including the MSE, mean absolute error (MAE), and root mean square error (RMSE) for the simulated and actual voltage-current characteristics at operating conditions of 1/1-bar and 343.15 K.

The error metrics MSE and MAE are used to assess the accuracy and reliability of the parameter estimation. The MSE is defined by the average squared difference between the simulated and experimental voltage-current values, highlighting large deviations more strongly due to the square operation, whereas the MAE uses the absolute rather than the square to define the average difference between simulated and experimental values, providing a direct measure of overall predictive accuracy. In the same context, RMSE, which is the square root of the MSE, provides the error in the same units as the data, allowing for direct interpretation as reported in [22,32,33].

Table 4. The optimum parameters obtained for the PEMFC 250 W at a pressure of 1/1 bar and a temperature of 343.15 K, based on the HCLBES and other algorithms.

	Algorithm	η_1	η_2	η_3	η_4	λ	b	R_C	MSE	MAE	RMSE
Range-1	Proposed HCLBES	$-9.48\ \varepsilon^{-1}$	$2.89\ \varepsilon^{-3}$	$7.60\ \varepsilon^{-5}$	$-1.37\ \varepsilon^{-4}$	$1.40\ \varepsilon^{1}$	$1.60\ \varepsilon^{-2}$	$7.84\ \varepsilon^{-4}$	$1.10\ \varepsilon^{-2}$	$8.69\ \varepsilon^{-2}$	$1.05\ \varepsilon^{-1}$
	ASO	$-9.48\ \varepsilon^{-1}$	$2.89\ \varepsilon^{-3}$	$7.59\ \varepsilon^{-5}$	$-1.43\ \varepsilon^{-4}$	$1.75\ \varepsilon^{1}$	$2.27\ \varepsilon^{-2}$	$5.86\ \varepsilon^{-4}$	$1.90\ \varepsilon^{-2}$	$1.16\ \varepsilon^{-1}$	$1.37\ \varepsilon^{-1}$
	HHO	$-9.52\ \varepsilon^{-1}$	$2.88\ \varepsilon^{-3}$	$7.40\ \varepsilon^{-5}$	$-1.38\ \varepsilon^{-4}$	$1.40\ \varepsilon^{1}$	$1.61\ \varepsilon^{-2}$	$6.89\ \varepsilon^{-4}$	$1.11\ \varepsilon^{-2}$	$8.69\ \varepsilon^{-2}$	$1.05\ \varepsilon^{-1}$
	GWO	$-9.48\ \varepsilon^{-1}$	$2.89\ \varepsilon^{-3}$	$7.58\ \varepsilon^{-5}$	$-1.37\ \varepsilon^{-4}$	$1.40\ \varepsilon^{1}$	$1.60\ \varepsilon^{-2}$	$7.62\ \varepsilon^{-4}$	$1.11\ \varepsilon^{-2}$	$8.68\ \varepsilon^{-2}$	$1.05\ \varepsilon^{-1}$
	SSA	$-9.48\ \varepsilon^{-1}$	$2.89\ \varepsilon^{-3}$	$7.57\ \varepsilon^{-5}$	$-1.40\ \varepsilon^{-4}$	$1.40\ \varepsilon^{1}$	$1.66\ \varepsilon^{-2}$	$5.18\ \varepsilon^{-4}$	$1.15\ \varepsilon^{-2}$	$8.85\ \varepsilon^{-2}$	$1.07\ \varepsilon^{-1}$
	BES	$-9.48\ \varepsilon^{-1}$	$2.90\ \varepsilon^{-3}$	$7.60\ \varepsilon^{-5}$	$-1.37\ \varepsilon^{-4}$	$1.40\ \varepsilon^{1}$	$1.60\ \varepsilon^{-2}$	$7.84\ \varepsilon^{-4}$	$1.10\ \varepsilon^{-2}$	$8.69\ \varepsilon^{-2}$	$1.05\ \varepsilon^{-1}$
	VSDE [46]	$-9.47\ \varepsilon^{-1}$	$2.90\ \varepsilon^{-3}$	$7.63\ \varepsilon^{-5}$	$-1.37\ \varepsilon^{-4}$	$1.40\ \varepsilon^{1}$	$1.60\ \varepsilon^{-2}$	$7.84\ \varepsilon^{-4}$	$1.10\ \varepsilon^{-2}$	$8.69\ \varepsilon^{-2}$	$1.05\ \varepsilon^{-1}$
	ABC [46]	$-9.49\ \varepsilon^{-1}$	$2.89\ \varepsilon^{-3}$	$7.55\ \varepsilon^{-5}$	$-1.37\ \varepsilon^{-4}$	$1.40\ \varepsilon^{1}$	$1.60\ \varepsilon^{-2}$	$7.84\ \varepsilon^{-4}$	$1.10\ \varepsilon^{-2}$	$8.69\ \varepsilon^{-2}$	$1.05\ \varepsilon^{-1}$
	HABC [21]	$-9.49\ \varepsilon^{-1}$	$2.89\ \varepsilon^{-3}$	$7.56\ \varepsilon^{-5}$	$-1.37\ \varepsilon^{-4}$	$1.40\ \varepsilon^{1}$	$1.60\ \varepsilon^{-2}$	$7.84\ \varepsilon^{-4}$	$1.10\ \varepsilon^{-2}$	$8.69\ \varepsilon^{-2}$	$1.05\ \varepsilon^{-1}$
	ITHS [32]	$-9.45\ \varepsilon^{-1}$	$2.87\ \varepsilon^{-3}$	$7.54\ \varepsilon^{-5}$	$-1.32\ \varepsilon^{-4}$	$1.75\ \varepsilon^{1}$	$2.53\ \varepsilon^{-2}$	$6.66\ \varepsilon^{-4}$	$4.83\ \varepsilon^{-2}$	$1.34\ \varepsilon^{-1}$	$1.73\ \varepsilon^{-1}$
	MVO [22]	$-9.48\ \varepsilon^{-1}$	$2.90\ \varepsilon^{-3}$	$7.62\ \varepsilon^{-5}$	$-1.39\ \varepsilon^{-4}$	$1.40\ \varepsilon^{1}$	$1.63\ \varepsilon^{-2}$	$6.03\ \varepsilon^{-4}$	$1.13\ \varepsilon^{-2}$	$8.76\ \varepsilon^{-2}$	$1.06\ \varepsilon^{-1}$
	STLBO [55]	$-9.48\ \varepsilon^{-1}$	$2.90\ \varepsilon^{-3}$	$7.62\ \varepsilon^{-5}$	$-1.37\ \varepsilon^{-4}$	$1.40\ \varepsilon^{1}$	$1.60\ \varepsilon^{-2}$	$7.84\ \varepsilon^{-4}$	$1.10\ \varepsilon^{-2}$	$8.69\ \varepsilon^{-2}$	$1.05\ \varepsilon^{-1}$
	TLBO [55]	$-9.46\ \varepsilon^{-1}$	$2.87\ \varepsilon^{-3}$	$7.47\ \varepsilon^{-5}$	$-1.37\ \varepsilon^{-4}$	$1.40\ \varepsilon^{1}$	$1.60\ \varepsilon^{-2}$	$7.84\ \varepsilon^{-4}$	$1.10\ \varepsilon^{-2}$	$8.69\ \varepsilon^{-2}$	$1.05\ \varepsilon^{-1}$
	VSA [46]	$-9.47\ \varepsilon^{-1}$	$2.95\ \varepsilon^{-3}$	$7.64\ \varepsilon^{-5}$	$-1.55\ \varepsilon^{-4}$	$1.40\ \varepsilon^{1}$	$2.47\ \varepsilon^{-2}$	$5.15\ \varepsilon^{-4}$	$7.27\ \varepsilon^{-1}$	$2.79\ \varepsilon^{-2}$	$3.69\ \varepsilon^{-1}$
	HCLAOA [20]	$-9.48\ \varepsilon^{-1}$	$2.91\ \varepsilon^{-3}$	$7.59\ \varepsilon^{-5}$	$-1.20\ \varepsilon^{-4}$	$1.99\ \varepsilon^{1}$	$4.76\ \varepsilon^{-2}$	$5.19\ \varepsilon^{-4}$	$5.93\ \varepsilon^{-1}$	$3.85\ \varepsilon^{-1}$	$5.39\ \varepsilon^{-1}$
Range-2	Proposed HCLBES	-1.03	$3.02\ \varepsilon^{-3}$	$6.69\ \varepsilon^{-5}$	$-1.37\ \varepsilon^{-4}$	$1.21\ \varepsilon^{1}$	$1.36\ \varepsilon^{-2}$	$1.00\ \varepsilon^{-4}$	$4.09\ \varepsilon^{-2}$	$1.41\ \varepsilon^{-1}$	$2.02\ \varepsilon^{-1}$
	ASO	-1.01	$2.99\ \varepsilon^{-3}$	$7.08\ \varepsilon^{-5}$	$-1.42\ \varepsilon^{-4}$	$1.70\ \varepsilon^{1}$	$2.16\ \varepsilon^{-2}$	$5.78\ \varepsilon^{-4}$	$4.46\ \varepsilon^{-2}$	$1.51\ \varepsilon^{-1}$	$2.07\ \varepsilon^{-1}$
	HHO	-1.03	$2.65\ \varepsilon^{-3}$	$3.87\ \varepsilon^{-5}$	$-1.32\ \varepsilon^{-4}$	$1.24\ \varepsilon^{1}$	$1.36\ \varepsilon^{-2}$	$5.37\ \varepsilon^{-4}$	$4.12\ \varepsilon^{-2}$	$1.41\ \varepsilon^{-1}$	$2.03\ \varepsilon^{-1}$
	GWO	-1.05	$3.04\ \varepsilon^{-3}$	$6.42\ \varepsilon^{-5}$	$-1.36\ \varepsilon^{-4}$	$1.24\ \varepsilon^{1}$	$1.37\ \varepsilon^{-2}$	$3.42\ \varepsilon^{-4}$	$4.11\ \varepsilon^{-2}$	$1.41\ \varepsilon^{-1}$	$2.03\ \varepsilon^{-1}$
	SSA	-1.02	$2.88\ \varepsilon^{-3}$	$5.99\ \varepsilon^{-5}$	$-1.36\ \varepsilon^{-4}$	$1.27\ \varepsilon^{1}$	$1.39\ \varepsilon^{-2}$	$4.48\ \varepsilon^{-4}$	$4.21\ \varepsilon^{-2}$	$1.46\ \varepsilon^{-1}$	$2.05\ \varepsilon^{-1}$
	BES	-1.02	$2.99\ \varepsilon^{-3}$	$6.71\ \varepsilon^{-5}$	$-1.36\ \varepsilon^{-4}$	$1.22\ \varepsilon^{1}$	$1.36\ \varepsilon^{-2}$	$1.68\ \varepsilon^{-4}$	$4.09\ \varepsilon^{-2}$	$1.41\ \varepsilon^{-1}$	$2.02\ \varepsilon^{-1}$
	VSDE [46]	-1.06	$3.23\ \varepsilon^{-3}$	$7.78\ \varepsilon^{-5}$	$-1.37\ \varepsilon^{-4}$	$1.20\ \varepsilon^{1}$	$1.36\ \varepsilon^{-2}$	$1.02\ \varepsilon^{-4}$	$4.09\ \varepsilon^{-2}$	$1.41\ \varepsilon^{-1}$	$2.02\ \varepsilon^{-1}$
	ABC [46]	-1.00	$3.02\ \varepsilon^{-3}$	$7.41\ \varepsilon^{-5}$	$-1.37\ \varepsilon^{-4}$	$1.24\ \varepsilon^{1}$	$1.38\ \varepsilon^{-2}$	$2.55\ \varepsilon^{-4}$	$4.09\ \varepsilon^{-2}$	$1.41\ \varepsilon^{-1}$	$2.02\ \varepsilon^{-1}$
	HABC [21]	-1.11	$3.06\ \varepsilon^{-3}$	$5.32\ \varepsilon^{-5}$	$-1.36\ \varepsilon^{-4}$	$1.22\ \varepsilon^{1}$	$1.37\ \varepsilon^{-2}$	$1.61\ \varepsilon^{-4}$	$4.09\ \varepsilon^{-2}$	$1.41\ \varepsilon^{-1}$	$2.02\ \varepsilon^{-1}$
	ITHS [32]	$-9.62\ \varepsilon{-}1$	$2.93\ \varepsilon^{-3}$	$7.66\ \varepsilon^{-5}$	$-1.33\ \varepsilon^{-4}$	$1.68\ \varepsilon^{1}$	$2.33\ \varepsilon^{-2}$	$5.66\ \varepsilon^{-4}$	$4.88\ \varepsilon^{-2}$	$1.66\ \varepsilon^{-1}$	$2.12\ \varepsilon^{-1}$
	MVO [22]	-1.04	$2.97\ \varepsilon^{-3}$	$6.24\ \varepsilon^{-5}$	$-1.36\ \varepsilon^{-4}$	$1.25\ \varepsilon^{1}$	$1.36\ \varepsilon^{-2}$	$3.95\ \varepsilon^{-4}$	$4.20\ \varepsilon^{-2}$	$1.45\ \varepsilon^{-1}$	$2.05\ \varepsilon^{-1}$
	STLBO [55]	-1.06	$3.05\ \varepsilon^{-3}$	$6.24\ \varepsilon^{-5}$	$-1.37\ \varepsilon^{-4}$	$1.21\ \varepsilon^{1}$	$1.36\ \varepsilon^{-2}$	$1.00\ \varepsilon^{-4}$	$4.09\ \varepsilon^{-2}$	$1.41\ \varepsilon^{-1}$	$2.02\ \varepsilon^{-1}$
	TLBO [55]	$-8.71\ \varepsilon{-}1$	$2.21\ \varepsilon^{-3}$	$3.98\ \varepsilon^{-5}$	$-1.37\ \varepsilon^{-4}$	$1.21\ \varepsilon^{1}$	$1.36\ \varepsilon^{-2}$	$1.00\ \varepsilon^{-4}$	$4.09\ \varepsilon^{-2}$	$1.41\ \varepsilon^{-1}$	$2.02\ \varepsilon^{-1}$
	VSA [46]	$-8.57\ \varepsilon{-}1$	$2.65\ \varepsilon^{-3}$	$7.49\ \varepsilon^{-5}$	$-9.73\ \varepsilon^{-5}$	$1.00\ \varepsilon^{1}$	$2.45\ \varepsilon^{-2}$	$3.96\ \varepsilon^{-4}$	1.10	$4.94\ \varepsilon^{-1}$	$6.02\ \varepsilon^{-1}$
	HCLAOA [20]	-1.02	$3.02\ \varepsilon^{-3}$	$6.14\ \varepsilon^{-5}$	$-1.64\ \varepsilon^{-4}$	$2.05\ \varepsilon^{1}$	$4.89\ \varepsilon^{-2}$	$4.61\ \varepsilon^{-4}$	$3.20\ \varepsilon^{-1}$	$3.16\ \varepsilon^{-1}$	$3.79\ \varepsilon^{-1}$

Scientific notation ε^n refers to 1×10^n, where n is a real integer value.

The results in Table 4 show that the HCLBES algorithm performs better than others in both operating ranges, achieving the lowest values for MSE, MAE, and RMSE. Notably, it outperforms other metaheuristic techniques in optimizing PEMFC parameters under specified conditions. This evidence indicates its strong capability in accurately estimating model coefficients with minimal error. The consistency of results across different performance metrics reinforces the robustness and reliability of the proposed HCLBES approach.

Among the algorithms tested, HCLBES performed the best, showing the lowest error values: MSE 2.0632 $\times 10^{-6}$, MAE 13 $\times 10^{-3}$, and RMSE 14 $\times 10^{-3}$, operating in range 1, indicating that the model performs more accurately and reliably in range 2. In addition, Table 5 compares seven estimated parameters, MSE, MAE, and RMSE for the operating conditions of 3/5 bar at 353.15 K (the pressures and temperature of the anode and cathode). In two different operating ranges, the proposed HCLBES algorithm consistently achieves the lowest RMSE and MAE values, indicating accurate prediction. The robustness of HCLBES across varying pressure and temperature conditions demonstrates its adaptability to different operating environments.

The results in Table 4 (at 1/1 bar and 343.15 K) show that the HCLBES algorithm, along with similar methods, consistently produces very small prediction errors. In Table 5 (at 3/5 bar and 353.15 K), the proposed HCLBES algorithm continues to deliver robust performance with low RMSE and MAE, even as the parameter values adjust to more demanding operating conditions. Together, these tables underscore the adaptability and high accuracy of HCLBES across varied pressures and temperature ranges in PEMFC modelling. In order to further assess the performance of the proposed HCLBES algorithm, a statistical evaluation was carried out over 30 separate tests, and the results are shown in Tables 6 and 7 for two situations: 1/1 bar at 343.15 K, and 3/5 bar at 353.15 K.

In this assessment, the key performance metrics, including the best, worst, mean, median, variance, and standard deviation of MSE values, were computed. The statistical analysis in Table 6 demonstrates that the proposed HCLBES algorithm achieved better performance than its counterparts, with much lower variability and standard deviation values. It clearly reveals that the proposed HCLBES algorithm achieves standard deviations as low as 1×10^{-15} to 1×10^{-5}. In contrast, other algorithms like ASO and SSA exhibit much higher deviations in the range of 1×10^{-3} to 1×10^{-4}, indicating less stability. The consistent performance of HCLBES across both operating ranges highlights its robustness and reliability in optimization tasks.

Table 7 shows that the proposed HCLBES algorithm consistently achieves the lowest standard deviation (as low as 1×10^{-15} to 1×10^{-11}), indicating exceptional stability under the 3/5 bar and 353.15 K conditions. The comparative proposed HCLBES among algorithms such as ASO and HHO displays much higher variability, with standard deviations in range of 1×10^{-3} to 1×10^{-5}. The near-identical best, worst, and average values for HCLBES further confirm its robustness and convergence reliability.

Tables 6 and 7 collectively reveal the better performance achieved by the proposed HCLBES algorithm across varying operating conditions.

The utilize of subgroup-based learning and a competitive learning mechanism enabled the proposed HCLBES to successfully avoid local optima and enhance convergence stability in order to reach a solution. These results validate HCLBES as highly reliable and accurate optimization method for PEMFC modelling across diverse scenarios.

Table 5. The optimum parameters obtained for the PEMFC 250 W at a pressure of 3/5 bar and a temperature of 353.15 K, based on the HCLBES and other algorithms.

	Algorithm	η_1	η_2	η_3	η_4	λ	b	R_C	MSE	MAE	RMSE
Range-1	Proposed HCLBES	$-9.48\ \varepsilon^{-1}$	$2.81\ \varepsilon^{-3}$	$7.63\ \varepsilon^{-5}$	$-1.21\ \varepsilon^{-4}$	$2.30\ \varepsilon^{+1}$	$6.25\ \varepsilon^{-2}$	$1.00\ \varepsilon^{-4}$	$1.00\ \varepsilon^{-2}$	$8.17\ \varepsilon^{-2}$	$1.00\ \varepsilon^{-1}$
	ASO	$-9.48\ \varepsilon^{-1}$	$2.81\ \varepsilon^{-3}$	$7.59\ \varepsilon^{-5}$	$-1.16\ \varepsilon^{-4}$	$1.98\ \varepsilon^{+1}$	$6.02\ \varepsilon^{-2}$	$1.17\ \varepsilon^{-4}$	$1.78\ \varepsilon^{-2}$	$1.18\ \varepsilon^{-1}$	$1.38\ \varepsilon^{-1}$
	HHO	$-9.44\ \varepsilon^{-1}$	$2.78\ \varepsilon^{-3}$	$7.52\ \varepsilon^{-5}$	$-1.20\ \varepsilon^{-4}$	$2.28\ \varepsilon^{+1}$	$6.22\ \varepsilon^{-2}$	$1.38\ \varepsilon^{-4}$	$1.11\ \varepsilon^{-2}$	$8.53\ \varepsilon^{-2}$	$1.03\ \varepsilon^{-1}$
	GWO	$-9.48\ \varepsilon^{-1}$	$2.80\ \varepsilon^{-3}$	$7.58\ \varepsilon^{-5}$	$-1.20\ \varepsilon^{-4}$	$2.30\ \varepsilon^{+1}$	$6.22\ \varepsilon^{-2}$	$1.78\ \varepsilon^{-4}$	$1.02\ \varepsilon^{-2}$	$8.14\ \varepsilon^{-2}$	$1.01\ \varepsilon^{-1}$
	SSA	$-9.48\ \varepsilon^{-1}$	$2.81\ \varepsilon^{-3}$	$7.63\ \varepsilon^{-5}$	$-1.18\ \varepsilon^{-4}$	$2.30\ \varepsilon^{+1}$	$6.13\ \varepsilon^{-2}$	$4.29\ \varepsilon^{-4}$	$1.04\ \varepsilon^{-2}$	$8.19\ \varepsilon^{-2}$	$1.02\ \varepsilon^{-1}$
	BES	$-9.48\ \varepsilon^{-1}$	$2.81\ \varepsilon^{-3}$	$7.60\ \varepsilon^{-5}$	$-1.21\ \varepsilon^{-4}$	$2.30\ \varepsilon^{+1}$	$6.25\ \varepsilon^{-2}$	$1.00\ \varepsilon^{-4}$	$1.01\ \varepsilon^{-2}$	$8.16\ \varepsilon^{-2}$	$1.00\ \varepsilon^{-1}$
	VSDE [46]	$-9.49\ \varepsilon^{-1}$	$2.81\ \varepsilon^{-3}$	$7.61\ \varepsilon^{-5}$	$-1.21\ \varepsilon^{-4}$	$2.30\ \varepsilon^{+1}$	$6.25\ \varepsilon^{-2}$	$1.00\ \varepsilon^{-4}$	$1.00\ \varepsilon^{-2}$	$8.19\ \varepsilon^{-2}$	$1.00\ \varepsilon^{-1}$
	ABC [46]	$-9.47\ \varepsilon^{-1}$	$2.82\ \varepsilon^{-3}$	$7.68\ \varepsilon^{-5}$	$-1.21\ \varepsilon^{-4}$	$2.30\ \varepsilon^{+1}$	$6.25\ \varepsilon^{-2}$	$1.00\ \varepsilon^{-4}$	$1.03\ \varepsilon^{-2}$	$8.13\ \varepsilon^{-2}$	$1.01\ \varepsilon^{-1}$
	HABC [21]	$-9.48\ \varepsilon^{-1}$	$2.81\ \varepsilon^{-3}$	$7.63\ \varepsilon^{-5}$	$-1.21\ \varepsilon^{-4}$	$2.30\ \varepsilon^{+1}$	$6.25\ \varepsilon^{-2}$	$1.00\ \varepsilon^{-4}$	$1.02\ \varepsilon^{-2}$	$8.20\ \varepsilon^{-2}$	$1.00\ \varepsilon^{-1}$
	ITHS [32]	$-9.45\ \varepsilon^{-1}$	$2.79\ \varepsilon^{-3}$	$7.55\ \varepsilon^{-5}$	$-1.11\ \varepsilon^{-4}$	$2.20\ \varepsilon^{+1}$	$6.18\ \varepsilon^{-2}$	$4.69\ \varepsilon^{-4}$	$4.16\ \varepsilon^{-2}$	$1.43\ \varepsilon^{-1}$	$1.81\ \varepsilon^{-1}$
	MVO [22]	$-9.49\ \varepsilon^{-1}$	$2.81\ \varepsilon^{-3}$	$7.61\ \varepsilon^{-5}$	$-1.18\ \varepsilon^{-4}$	$2.30\ \varepsilon^{+1}$	$6.15\ \varepsilon^{-2}$	$3.86\ \varepsilon^{-4}$	$1.02\ \varepsilon^{-2}$	$8.15\ \varepsilon^{-2}$	$1.01\ \varepsilon^{-1}$
	STLBO [55]	$-9.49\ \varepsilon^{-1}$	$2.81\ \varepsilon^{-3}$	$7.61\ \varepsilon^{-5}$	$-1.21\ \varepsilon^{-4}$	$2.30\ \varepsilon^{+1}$	$6.25\ \varepsilon^{-2}$	$1.00\ \varepsilon^{-4}$	$1.00\ \varepsilon^{-2}$	$8.17\ \varepsilon^{-2}$	$1.00\ \varepsilon^{-1}$
	TLBO [55]	$-9.47\ \varepsilon^{-1}$	$2.79\ \varepsilon^{-3}$	$7.55\ \varepsilon^{-5}$	$-1.21\ \varepsilon^{-4}$	$2.30\ \varepsilon^{+1}$	$6.25\ \varepsilon^{-2}$	$1.00\ \varepsilon^{-4}$	$1.00\ \varepsilon^{-2}$	$8.17\ \varepsilon^{-2}$	$1.00\ \varepsilon^{-1}$
	VSA [46]	$-9.46\ \varepsilon^{-1}$	$2.86\ \varepsilon^{-3}$	$7.59\ \varepsilon^{-5}$	$-1.68\ \varepsilon^{-4}$	$1.40\ \varepsilon^{+1}$	$2.80\ \varepsilon^{-2}$	$3.83\ \varepsilon^{-4}$	1.05	$3.98\ \varepsilon^{-1}$	$4.58\ \varepsilon^{-1}$
	HCLAOA [20]	$-9.48\ \varepsilon^{-1}$	$2.84\ \varepsilon^{-3}$	$7.63\ \varepsilon^{-5}$	$-1.03\ \varepsilon^{-4}$	$2.10\ \varepsilon^{+1}$	$7.35\ \varepsilon^{-2}$	$4.63\ \varepsilon^{-4}$	1.47	$6.12\ \varepsilon^{-1}$	$8.01\ \varepsilon^{-1}$
Range-2	Proposed HCLBES	-1.02	$2.97\ \varepsilon^{-3}$	$7.21\ \varepsilon^{-5}$	$-1.22\ \varepsilon^{-4}$	$2.40\ \varepsilon^{+1}$	$6.31\ \varepsilon^{-2}$	$1.00\ \varepsilon^{-4}$	$4.07\ \varepsilon^{-2}$	$1.40\ \varepsilon^{-1}$	$2.02\ \varepsilon^{-1}$
	ASO	-1.02	$2.91\ \varepsilon^{-3}$	$6.83\ \varepsilon^{-5}$	$-1.17\ \varepsilon^{-4}$	$1.98\ \varepsilon^{+1}$	$5.79\ \varepsilon^{-2}$	$2.77\ \varepsilon^{-4}$	$4.56\ \varepsilon^{-2}$	$1.45\ \varepsilon^{-1}$	$2.13\ \varepsilon^{-1}$
	HHO	-1.06	$3.35\ \varepsilon^{-3}$	$9.18\ \varepsilon^{-5}$	$-1.16\ \varepsilon^{-4}$	$2.29\ \varepsilon^{+1}$	$6.04\ \varepsilon^{-2}$	$5.83\ \varepsilon^{-4}$	$4.42\ \varepsilon^{-2}$	$1.47\ \varepsilon^{-1}$	$2.08\ \varepsilon^{-1}$
	GWO	-1.05	$2.79\ \varepsilon^{-3}$	$5.46\ \varepsilon^{-5}$	$-1.21\ \varepsilon^{-4}$	$2.40\ \varepsilon^{+1}$	$6.26\ \varepsilon^{-2}$	$2.20\ \varepsilon^{-4}$	$4.10\ \varepsilon^{-2}$	$1.40\ \varepsilon^{-1}$	$2.02\ \varepsilon^{-1}$
	SSA	-1.04	$2.93\ \varepsilon^{-3}$	$6.57\ \varepsilon^{-5}$	$-1.18\ \varepsilon^{-4}$	$2.35\ \varepsilon^{+1}$	$6.14\ \varepsilon^{-2}$	$4.70\ \varepsilon^{-4}$	$4.20\ \varepsilon^{-2}$	$1.45\ \varepsilon^{-1}$	$2.05\ \varepsilon^{-1}$
	BES	-1.01	$2.86\ \varepsilon^{-3}$	$6.73\ \varepsilon^{-5}$	$-1.22\ \varepsilon^{-4}$	$2.40\ \varepsilon^{+1}$	$6.31\ \varepsilon^{-2}$	$1.01\ \varepsilon^{-4}$	$4.07\ \varepsilon^{-2}$	$1.40\ \varepsilon^{-1}$	$2.02\ \varepsilon^{-1}$
	VSDE [46]	-1.09	$3.30\ \varepsilon^{-3}$	$8.11\ \varepsilon^{-5}$	$-1.22\ \varepsilon^{-4}$	$2.40\ \varepsilon^{+1}$	$6.31\ \varepsilon^{-2}$	$1.00\ \varepsilon^{-4}$	$4.07\ \varepsilon^{-2}$	$1.40\ \varepsilon^{-1}$	$2.02\ \varepsilon^{-1}$
	ABC [46]	-1.05	$2.91\ \varepsilon^{-3}$	$6.10\ \varepsilon^{-5}$	$-1.22\ \varepsilon^{-4}$	$2.40\ \varepsilon^{+1}$	$6.31\ \varepsilon^{-2}$	$1.00\ \varepsilon^{-4}$	$4.07\ \varepsilon^{-2}$	$1.40\ \varepsilon^{-1}$	$2.02\ \varepsilon^{-1}$
	HABC [21]	-1.06	$2.95\ \varepsilon^{-3}$	$6.24\ \varepsilon^{-5}$	$-1.22\ \varepsilon^{-4}$	$2.40\ \varepsilon^{+1}$	$6.31\ \varepsilon^{-2}$	$1.03\ \varepsilon^{-4}$	$4.07\ \varepsilon^{-2}$	$1.40\ \varepsilon^{-1}$	$2.02\ \varepsilon^{-1}$
	ITHS [32]	$-9.51\ \varepsilon^{-1}$	$2.82\ \varepsilon^{-3}$	$7.66\ \varepsilon^{-5}$	$-1.14\ \varepsilon^{-4}$	$2.20\ \varepsilon^{+1}$	$6.14\ \varepsilon^{-2}$	$4.66\ \varepsilon^{-4}$	$5.55\ \varepsilon^{-2}$	$1.58\ \varepsilon^{-1}$	$2.09\ \varepsilon^{-1}$
	MVO [22]	-1.03	$2.87\ \varepsilon^{-3}$	$6.40\ \varepsilon^{-5}$	$-1.19\ \varepsilon^{-4}$	$2.38\ \varepsilon^{+1}$	$6.20\ \varepsilon^{-2}$	$3.68\ \varepsilon^{-4}$	$4.16\ \varepsilon^{-2}$	$1.43\ \varepsilon^{-1}$	$2.04\ \varepsilon^{-1}$
	STLBO [55]	-1.00	$2.92\ \varepsilon^{-3}$	$7.20\ \varepsilon^{-5}$	$-1.22\ \varepsilon^{-4}$	$2.40\ \varepsilon^{+1}$	$6.31\ \varepsilon^{-2}$	$1.00\ \varepsilon^{-4}$	$4.07\ \varepsilon^{-2}$	$1.40\ \varepsilon^{-1}$	$2.02\ \varepsilon^{-1}$
	TLBO [55]	$-8.70\ \varepsilon^{-1}$	$2.22\ \varepsilon^{-3}$	$5.06\ \varepsilon^{-5}$	$-1.22\ \varepsilon^{-4}$	$2.40\ \varepsilon^{+1}$	$6.31\ \varepsilon^{-2}$	$1.00\ \varepsilon^{-4}$	$4.07\ \varepsilon^{-2}$	$1.40\ \varepsilon^{-1}$	$2.02\ \varepsilon^{-1}$
	VSA [46]	$-8.58\ \varepsilon^{-1}$	$2.60\ \varepsilon^{-3}$	$7.73\ \varepsilon^{-5}$	$-1.15\ \varepsilon^{-4}$	$1.00\ \varepsilon^{+1}$	$2.90\ \varepsilon^{-2}$	$4.49\ \varepsilon^{-4}$	$8.41\ \varepsilon^{-2}$	$3.41\ \varepsilon^{-1}$	$4.46\ \varepsilon^{-1}$
	HCLAOA [20]	-1.04	$3.07\ \varepsilon^{-3}$	$6.81\ \varepsilon^{-5}$	$-1.52\ \varepsilon^{-4}$	$2.30\ \varepsilon^{+1}$	$6.78\ \varepsilon^{-2}$	$3.75\ \varepsilon^{-4}$	$5.05\ \varepsilon^{-2}$	$4.59\ \varepsilon^{-1}$	$5.42\ \varepsilon^{-1}$

Scientific notation ε^n refers to 1×10^n, where n is a real integer value.

Table 6. Statistical analysis of the proposed HCLBES and other counterparts of the PEMFC 250 W model corresponding to an operating condition of 1/1 bar at 343.15 K.

	Algorithm	Best	Worst	Aver	Median	Var	Std
Range-1	Proposed HCLBES	$1.10\ \varepsilon^{-2}$	$1.10\ \varepsilon^{-2}$	$1.10\ \varepsilon^{-2}$	$1.10\ \varepsilon^{-2}$	$1.43\ \varepsilon^{-29}$	$3.77\ \varepsilon^{-15}$
	ASO	$1.14\ \varepsilon^{-2}$	$2.61\ \varepsilon^{-2}$	$1.90\ \varepsilon^{-2}$	$1.93\ \varepsilon^{-2}$	$1.45\ \varepsilon^{-5}$	$3.80\ \varepsilon^{-3}$
	HHO	$1.10\ \varepsilon^{-2}$	$1.15\ \varepsilon^{-2}$	$1.11\ \varepsilon^{-2}$	$1.10\ \varepsilon^{-2}$	$2.92\ \varepsilon^{-8}$	$1.71\ \varepsilon^{-4}$
	GWO	$1.10\ \varepsilon^{-2}$	$1.19\ \varepsilon^{-2}$	$1.11\ \varepsilon^{-2}$	$1.10\ \varepsilon^{-2}$	$2.72\ \varepsilon^{-8}$	$1.65\ \varepsilon^{-4}$
	SSA	$1.10\ \varepsilon^{-2}$	$1.29\ \varepsilon^{-2}$	$1.15\ \varepsilon^{-2}$	$1.15\ \varepsilon^{-2}$	$2.53\ \varepsilon^{-7}$	$5.03\ \varepsilon^{-4}$
	BES	$1.10\ \varepsilon^{-2}$	$1.10\ \varepsilon^{-2}$	$1.10\ \varepsilon^{-2}$	$1.10\ \varepsilon^{-2}$	$5.68\ \varepsilon^{-17}$	$7.54\ \varepsilon^{-9}$
Range-2	Proposed HCLBES	$1.00\ \varepsilon^{-2}$	$1.01\ \varepsilon^{-2}$	$1.00\ \varepsilon^{-2}$	$1.00\ \varepsilon^{-2}$	$1.23\ \varepsilon^{-10}$	$1.11\ \varepsilon^{-5}$
	ASO	$1.10\ \varepsilon^{-2}$	$2.70\ \varepsilon^{-2}$	$1.78\ \varepsilon^{-2}$	$1.78\ \varepsilon^{-2}$	$2.32\ \varepsilon^{-5}$	$4.82\ \varepsilon^{-3}$
	HHO	$1.03\ \varepsilon^{-2}$	$1.75\ \varepsilon^{-2}$	$1.11\ \varepsilon^{-2}$	$1.03\ \varepsilon^{-2}$	$3.08\ \varepsilon^{-6}$	$1.76\ \varepsilon^{-3}$
	GWO	$1.00\ \varepsilon^{-2}$	$1.06\ \varepsilon^{-2}$	$1.02\ \varepsilon^{-2}$	$1.01\ \varepsilon^{-2}$	$2.23\ \varepsilon^{-8}$	$1.49\ \varepsilon^{-4}$
	SSA	$1.00\ \varepsilon^{-2}$	$1.37\ \varepsilon^{-2}$	$1.04\ \varepsilon^{-2}$	$1.03\ \varepsilon^{-2}$	$4.28\ \varepsilon^{-7}$	$6.54\ \varepsilon^{-4}$
	BES	$1.00\ \varepsilon^{-2}$	$1.04\ \varepsilon^{-2}$	$1.01\ \varepsilon^{-2}$	$1.00\ \varepsilon^{-2}$	$9.51\ \varepsilon^{-9}$	$9.75\ \varepsilon^{-5}$

Scientific notation ε^n refers to 1×10^n, where n is a real integer value.

Table 7. Statistical analysis of the proposed HCLBES and other counterparts of the PEMFC 250 W model corresponding to an operating condition of 3/5 bar at 353.15 K.

	Algorithm	Best	Worst	Aver	Median	Var	Std
Range-1	Proposed HCLBES	$4.09\ \varepsilon^{-2}$	$4.09\ \varepsilon^{-2}$	$4.09\ \varepsilon^{-2}$	$4.09\ \varepsilon^{-2}$	$8.09\ \varepsilon^{-30}$	2.84 E ε^{-15}
	ASO	$4.13\ \varepsilon^{-2}$	$5.45\ \varepsilon^{-2}$	$4.46\ \varepsilon^{-2}$	$4.37\ \varepsilon^{-2}$	$9.47\ \varepsilon^{-6}$	$3.08\ \varepsilon^{-3}$
	HHO	$4.09\ \varepsilon^{-2}$	$4.23\ \varepsilon^{-2}$	$4.12\ \varepsilon^{-2}$	$4.10\ \varepsilon^{-2}$	$1.56\ \varepsilon^{-7}$	$3.95\ \varepsilon^{-4}$
	GWO	$4.09\ \varepsilon^{-2}$	$4.18\ \varepsilon^{-2}$	$4.11\ \varepsilon^{-2}$	$4.11\ \varepsilon^{-2}$	$6.60\ \varepsilon^{-8}$	$2.57\ \varepsilon^{-4}$
	SSA	$4.10\ \varepsilon^{-2}$	$4.29\ \varepsilon^{-2}$	$4.21\ \varepsilon^{-2}$	$4.20\ \varepsilon^{-2}$	$3.17\ \varepsilon^{-7}$	$5.63\ \varepsilon^{-4}$
	BES	$4.09\ \varepsilon^{-2}$	$4.09\ \varepsilon^{-2}$	$4.09\ \varepsilon^{-2}$	$4.09\ \varepsilon^{-2}$	$2.38\ \varepsilon^{-16}$	$1.54\ \varepsilon^{-8}$
Range-2	Proposed HCLBES	$4.0\ \varepsilon^{-2}$	$4.07\ \varepsilon^{-2}$	$4.07\ \varepsilon^{-2}$	$4.07\ \varepsilon^{-2}$	$1.84\ \varepsilon^{-22}$	$1.36\ \varepsilon^{-11}$
	ASO	$4.20\ \varepsilon^{-2}$	$5.62\ \varepsilon^{-2}$	$4.56\ \varepsilon^{-2}$	$4.48\ \varepsilon^{-2}$	$1.05\ \varepsilon^{-5}$	$3.24\ \varepsilon^{-3}$
	HHO	$4.20\ \varepsilon^{-2}$	$6.57\ \varepsilon^{-2}$	$4.42\ \varepsilon^{-2}$	$4.20\ \varepsilon^{-2}$	$2.66\ \varepsilon^{-5}$	$5.16\ \varepsilon^{-3}$
	GWO	$4.07\ \varepsilon^{-2}$	$4.24\ \varepsilon^{-2}$	$4.10\ \varepsilon^{-2}$	$4.08\ \varepsilon^{-2}$	$2.19\ \varepsilon^{-7}$	$4.68\ \varepsilon^{-4}$
	SSA	$4.09\ \varepsilon^{-2}$	$4.33\ \varepsilon^{-2}$	$4.20\ \varepsilon^{-2}$	$4.20\ \varepsilon^{-2}$	$2.95\ \varepsilon^{-7}$	$5.43\ \varepsilon^{-4}$
	BES	$4.07\ \varepsilon^{-2}$	$4.07\ \varepsilon^{-2}$	$4.07\ \varepsilon^{-2}$	$4.07\ \varepsilon^{-2}$	$1.85\ \varepsilon^{-10}$	$1.36\ \varepsilon^{-5}$

Scientific notation ε^n refers to 1×10^n, where n is a real integer value.

The convergence behavior of the proposed HCLBES was also compared against other algorithms, as shown in the average convergence curves in Figure 4a,b. Unlike ASO and HHO, which showed slower convergence and limited search efficiency, and BES and SSA, which tended to stagnate at higher MSE values, HCLBES maintained rapid and stable convergence in the optimization process. Such behaviour indicates a strong balance between exploration and exploitation throughout the optimization process. Consequently, the proposed HCLBES consistently achieved the lowest MSE across both PEMFC operating ranges.

The current–voltage characteristics of the PEMFC stack under two operating conditions are illustrated in Figure 5a,b. The HCLBES algorithm accurately tracks the experimental data, maintaining close alignment across the full current range. In addition to that, the estimated curves under both 1/1-bar 343.15 K and 3/5-bar 353.15 K conditions show minimal deviation from experimental results. The close agreement between experimental and predicted data across all scenarios confirms the effectiveness, robustness, and applicability of the proposed HCLBES algorithm for accurately modelling PEMFC behavior under varying conditions.

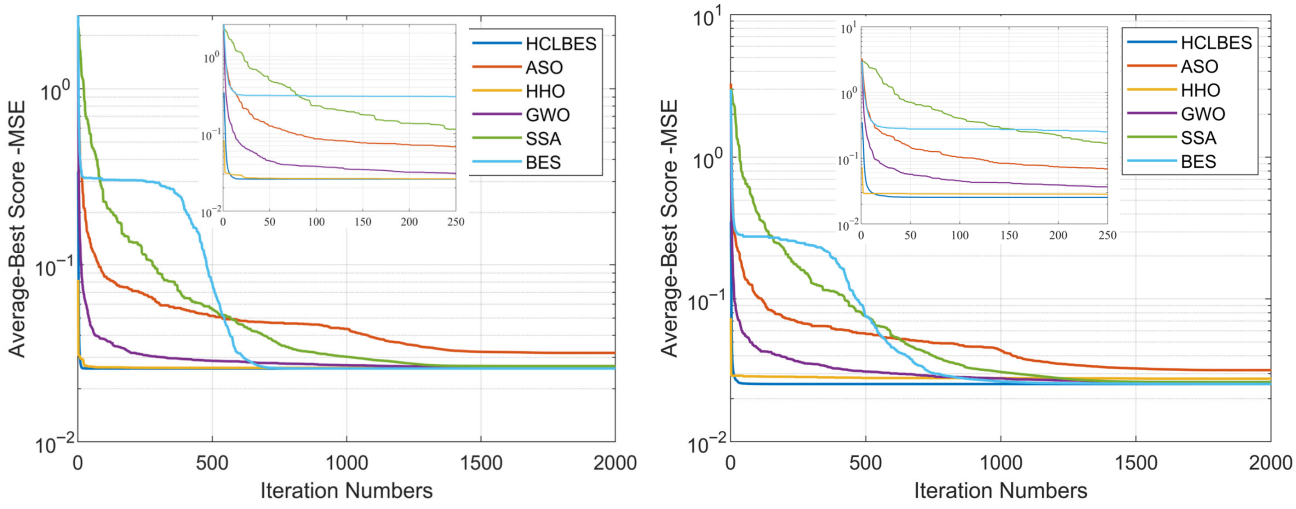


Figure 4. The average convergence curve for the proposed HCLBES and the other considered algorithms for the implemented cases of (**a**) Range-1, (**b**) Range-2 of PEMFC 250 W, corresponding to the two operating conditions of 1/1 bar at 343.15 K and 3/5 bar at 353.15 K.

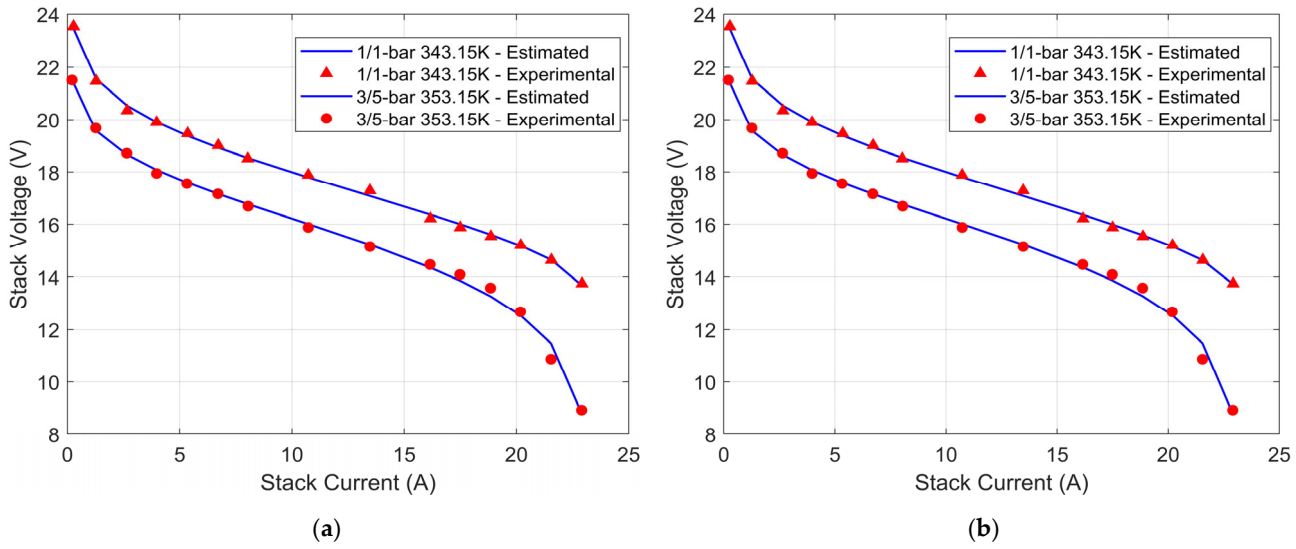


Figure 5. The current-voltage curve of the PEMFC 250 W stack for the proposed HCLBES for two implemented cases: (**a**) Range-1, (**b**) Range-2, which correspond to the operating conditions of 1/1 bar at 343.15 K and 3/5 bar at 353.15 K.

Figures 4 and 5 collectively demonstrated the effectiveness of HCLBES for modelling and optimizing PEMFC stack performance. Figure 4 highlights that the proposed HCLBES exhibits superior convergence behavior, achieving lower MSE values faster than its counterpart algorithms across both operating ranges. Meanwhile, Figure 5 confirmed the accuracy of the estimated model, with estimated polarization curves closely matching experimental data under different conditions. These results validate robustness, accuracy, and generalization capability of HCLBES for PEMFC system identification.

6.2. Parameter Identification for PEMFC 500 W Stack-Models

This subsection applies the proposed HCLBES to three different PEMFCs, each rated at 500 W: NedStack PS6, Horizon 500 W, and BCS 500 W. The corresponding electrical specifications for the three PEMFCs are detailed in Table 2. These datasets were chosen to validate PEMFC models because they are publicly available and contain a wide range of

operating conditions and performance measures. This makes them ideal for evaluating the accuracy and robustness of PEMFC models across a wide range of practical scenarios. The model parameter identification was performed using HCLBES and benchmarked against five other algorithms: ASO, HHO, GWO, SSA, and BES. Additionally, the performance was compared with values from recent literature employing WSO, MVO, VSDE, HBO, ALO, and HCLAOA algorithms.

Table 8 presents the identified parameters alongside their MSE, MAE, and RMS values. Among all the test algorithms, the proposed HCLBES consistently achieved the lowest MSE across the three PEMFCs, demonstrating superior performance while achieving the lowest error metrics (MSE, MAE, and RMSE) across all fuel cell systems tested. Meanwhile, it maintains high accuracy while preserving parameter stability and robustness under different operating conditions. Table 8 shows a thorough comparison of the proposed HCLBES and other algorithms across three PEMFC models under different conditions.

Table 9 provides the statistical evaluations, including best, worst, average, median, variance, and standard deviation values. The HCLBES consistently achieves the lowest, best, average, and worst error values with negligible variance and standard deviation, reflecting high reliability and accuracy. Competing algorithms like ASO and HHO show higher dispersion, indicating less consistent performance.

Convergence behaviour, depicted in Figure 6, illustrates the mean convergence curves performance of the proposed HCLBES algorithm compared to five benchmark optimizations across three PEMFC models. The HCLBES consistently achieves faster and more stable convergence, attaining the lowest MSE in all scenarios.

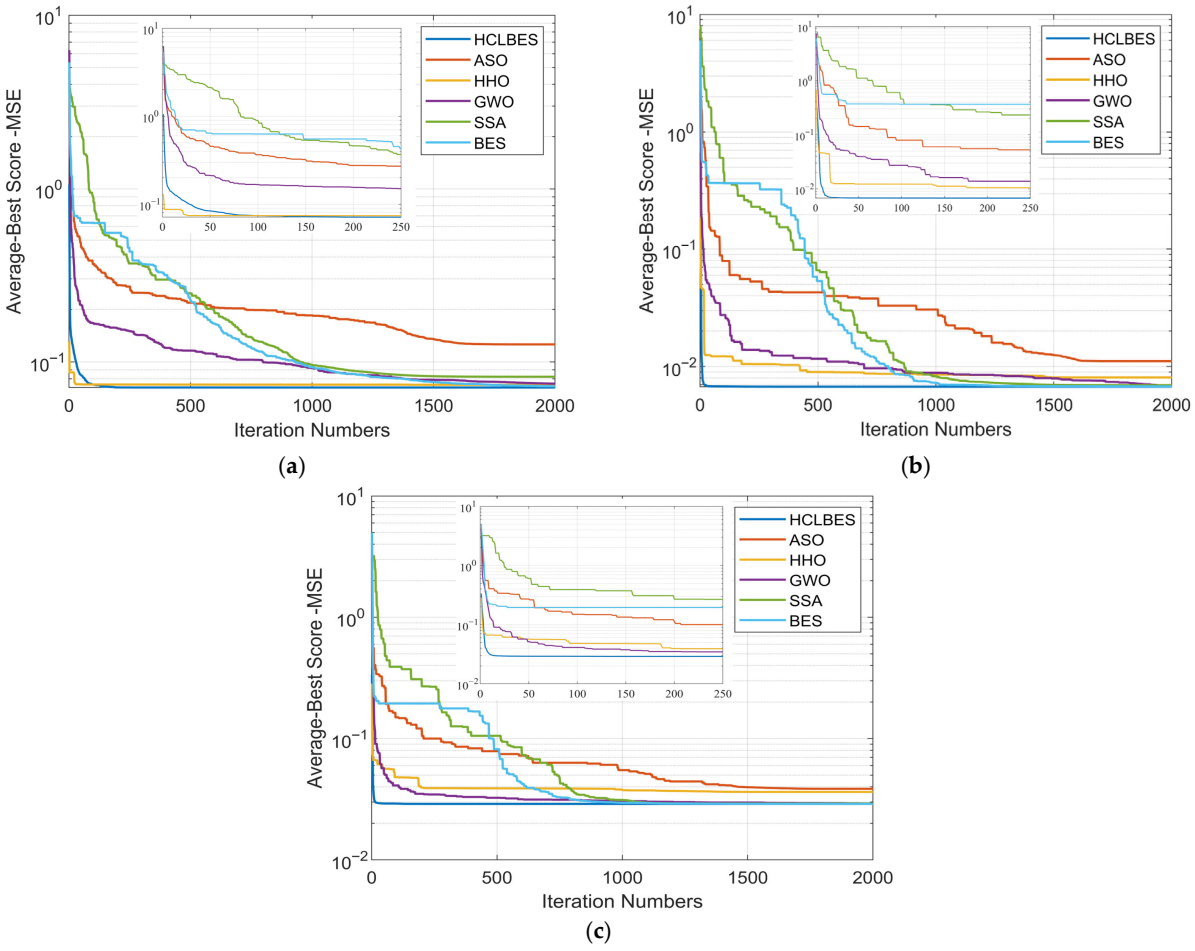


Figure 6. Comparison of average convergence across iterations for HCLBES and alternative algorithms applied to: (**a**) NedStack PS6 fuel cell, (**b**) Horizon 500 fuel cell, and (**c**) BCS 500 W fuel cell.

Table 8. The optimum parameter values for the 500 W PEMFC under different operating conditions, as estimated by HCLBES and other optimization algorithms.

	Algorithm	η_1	η_2	η_3	η_4	λ	b	R_C	MSE	MAE	RMSE
NedStack PS6—Model	Proposed HCLBES	−1.08	$3.54\,\varepsilon^{-3}$	$7.06\,\varepsilon^{-5}$	$-9.54\,\varepsilon^{-5}$	$1.26\,\varepsilon^{+1}$	$1.36\,\varepsilon^{-2}$	$1.00\,\varepsilon^{-4}$	$7.12\,\varepsilon^{-2}$	$2.05\,\varepsilon^{-1}$	$2.67\,\varepsilon^{-1}$
	ASO	−1.04	$3.43\,\varepsilon^{-3}$	$7.11\,\varepsilon^{-5}$	$-9.54\,\varepsilon^{-5}$	$1.72\,\varepsilon^{+1}$	$1.68\,\varepsilon^{-1}$	$2.41\,\varepsilon^{-4}$	$1.26\,\varepsilon^{-1}$	$3.10\,\varepsilon^{-1}$	$4.02\,\varepsilon^{-1}$
	HHO	$-8.53\,\varepsilon^{-1}$	$2.61\,\varepsilon^{-3}$	$5.07\,\varepsilon^{-5}$	$-9.54\,\varepsilon^{-5}$	$1.29\,\varepsilon^{+1}$	$3.95\,\varepsilon^{-2}$	$1.06\,\varepsilon^{-4}$	$7.38\,\varepsilon^{-2}$	$2.07\,\varepsilon^{-1}$	$2.71\,\varepsilon^{-1}$
	GWO	−1.03	$3.31\,\varepsilon^{-3}$	$6.36\,\varepsilon^{-5}$	$-9.54\,\varepsilon^{-5}$	$1.30\,\varepsilon^{+1}$	$5.43\,\varepsilon^{-2}$	$1.05\,\varepsilon^{-4}$	$7.49\,\varepsilon^{-2}$	$2.09\,\varepsilon^{-1}$	$2.73\,\varepsilon^{-1}$
	SSA	−1.03	$3.22\,\varepsilon^{-3}$	$5.71\,\varepsilon^{-5}$	$-9.54\,\varepsilon^{-5}$	$1.37\,\varepsilon^{+1}$	$1.15\,\varepsilon^{-1}$	$1.04\,\varepsilon^{-4}$	$8.21\,\varepsilon^{-2}$	$2.19\,\varepsilon^{-1}$	$2.94\,\varepsilon^{-1}$
	BES	−1.00	$3.24\,\varepsilon^{-3}$	$6.46\,\varepsilon^{-5}$	$-9.54\,\varepsilon^{-5}$	$1.27\,\varepsilon^{+1}$	$1.81\,\varepsilon^{-2}$	$1.04\,\varepsilon^{-4}$	$7.23\,\varepsilon^{-2}$	$2.06\,\varepsilon^{-1}$	$2.68\,\varepsilon^{-1}$
	WSO [23]	$-8.62\,\varepsilon^{-1}$	$3.05\,\varepsilon^{-3}$	$8.07\,\varepsilon^{-5}$	$-9.54\,\varepsilon^{-5}$	$1.26\,\varepsilon^{+1}$	$1.36\,\varepsilon^{-2}$	$1.00\,\varepsilon^{-4}$	$7.12\,\varepsilon^{-2}$	$2.05\,\varepsilon^{-1}$	$2.67\,\varepsilon^{-1}$
	MVO [22]	−1.01	$3.20\,\varepsilon^{-3}$	$6.10\,\varepsilon^{-5}$	$-9.54\,\varepsilon^{-5}$	$1.39\,\varepsilon^{+1}$	$1.38\,\varepsilon^{-1}$	$1.00\,\varepsilon^{-4}$	$8.33\,\varepsilon^{-2}$	$2.19\,\varepsilon^{-1}$	$2.90\,\varepsilon^{-1}$
	VSDE [46]	−1.09	$3.68\,\varepsilon^{-3}$	$7.86\,\varepsilon^{-5}$	$-9.54\,\varepsilon^{-5}$	$1.26\,\varepsilon^{+1}$	$1.40\,\varepsilon^{-2}$	$1.00\,\varepsilon^{-4}$	$7.13\,\varepsilon^{-2}$	$2.05\,\varepsilon^{-1}$	$2.67\,\varepsilon^{-1}$
	HBO [25]	−1.06	$3.54\,\varepsilon^{-3}$	$7.50\,\varepsilon^{-5}$	$-9.54\,\varepsilon^{-5}$	$1.2\,\varepsilon^{+1}$	$1.36\,\varepsilon^{-2}$	$1.01\,\varepsilon^{-4}$	$7.13\,\varepsilon^{-2}$	$2.05\,\varepsilon^{-1}$	$2.67\,\varepsilon^{-1}$
	ALO [24]	$-8.53\,\varepsilon^{-1}$	$2.41\,\varepsilon^{-3}$	$3.65\,\varepsilon^{-5}$	$-9.54\,\varepsilon^{-5}$	$1.29\,\varepsilon^{+1}$	$4.47\,\varepsilon^{-2}$	$1.00\,\varepsilon^{-4}$	$7.42\,\varepsilon^{-2}$	$2.06\,\varepsilon^{-1}$	$2.72\,\varepsilon^{-1}$
	HCLAOA [20]	−1.02	$3.42\,\varepsilon^{-3}$	$6.35\,\varepsilon^{-5}$	$-1.30\,\varepsilon^{-4}$	$1.97\,\varepsilon^{+1}$	$1.74\,\varepsilon^{-1}$	$2.67\,\varepsilon^{-4}$	1.03	$6.04\,\varepsilon^{-1}$	$8.64\,\varepsilon^{-1}$
Horizon 500—Model	Proposed HCLBES	−1.03	$3.22\,\varepsilon^{-3}$	$6.85\,\varepsilon^{-5}$	$-1.90\,\varepsilon^{-4}$	$2.17\,\varepsilon^{+1}$	$1.36\,\varepsilon^{-2}$	$8.00\,\varepsilon^{-4}$	$2.89\,\varepsilon^{-2}$	$1.33\,\varepsilon^{-1}$	$1.70\,\varepsilon^{-1}$
	ASO	−1.02	$3.18\,\varepsilon^{-3}$	$6.70\,\varepsilon^{-5}$	$-1.92\,\varepsilon^{-4}$	$1.95\,\varepsilon^{+1}$	$1.70\,\varepsilon^{-2}$	$1.61\,\varepsilon^{-4}$	$3.86\,\varepsilon^{-2}$	$1.41\,\varepsilon^{-1}$	$1.95\,\varepsilon^{-1}$
	HHO	−1.20	$3.49\,\varepsilon^{-3}$	$5.44\,\varepsilon^{-5}$	$-1.83\,\varepsilon^{-4}$	$1.52\,\varepsilon^{+1}$	$1.38\,\varepsilon^{-2}$	$1.38\,\varepsilon^{-4}$	$3.63\,\varepsilon^{-2}$	$1.36\,\varepsilon^{-1}$	$1.80\,\varepsilon^{-1}$
	GWO	−1.02	$3.09\,\varepsilon^{-3}$	$6.16\,\varepsilon^{-5}$	$-1.91\,\varepsilon^{-4}$	$1.95\,\varepsilon^{+1}$	$1.36\,\varepsilon^{-2}$	$5.21\,\varepsilon^{-4}$	$2.92\,\varepsilon^{-2}$	$1.31\,\varepsilon^{-1}$	$1.71\,\varepsilon^{-1}$
	SSA	−1.01	$3.23\,\varepsilon^{-3}$	$7.29\,\varepsilon^{-5}$	$-1.91\,\varepsilon^{-4}$	$1.93\,\varepsilon^{+1}$	$1.36\,\varepsilon^{-2}$	$5.15\,\varepsilon^{-4}$	$2.92\,\varepsilon^{-2}$	$1.32\,\varepsilon^{-1}$	$1.71\,\varepsilon^{-1}$
	BES	−1.03	$3.17\,\varepsilon^{-3}$	$6.61\,\varepsilon^{-5}$	$-1.90\,\varepsilon^{-4}$	$2.15\,\varepsilon^{+1}$	$1.36\,\varepsilon^{-2}$	$7.96\,\varepsilon^{-4}$	$2.90\,\varepsilon^{-2}$	$1.32\,\varepsilon^{-1}$	1.70 E−1
	WSO [23]	$-9.10\,\varepsilon^{-1}$	$3.31\,\varepsilon^{-3}$	$9.78\,\varepsilon^{-5}$	$-1.90\,\varepsilon^{-4}$	$2.17\,\varepsilon^{+1}$	$1.36\,\varepsilon^{-2}$	$8.00\,\varepsilon^{-4}$	$2.89\,\varepsilon^{-2}$	$1.33\,\varepsilon^{-1}$	$1.70\,\varepsilon^{-1}$
	MVO [22]	$-9.51\,\varepsilon^{-1}$	$2.91\,\varepsilon^{-3}$	$6.43\,\varepsilon^{-5}$	$-1.90\,\varepsilon^{-4}$	$1.91\,\varepsilon^{+1}$	$1.36\,\varepsilon^{-2}$	$5.05\,\varepsilon^{-4}$	$2.92\,\varepsilon^{-2}$	$1.32\,\varepsilon^{-1}$	$1.71\,\varepsilon^{-1}$
	VSDE [46]	−1.04	$3.28\,\varepsilon^{-3}$	$7.03\,\varepsilon^{-5}$	$-1.90\,\varepsilon^{-4}$	$2.15\,\varepsilon^{+1}$	$1.36\,\varepsilon^{-2}$	$7.89\,\varepsilon^{-4}$	$2.90\,\varepsilon^{-2}$	$1.33\,\varepsilon^{-1}$	$1.70\,\varepsilon^{-1}$
	HBO [25]	−1.12	$3.60\,\varepsilon^{-3}$	$7.60\,\varepsilon^{-5}$	$-1.90\,\varepsilon^{-4}$	$2.17\,\varepsilon^{+1}$	$1.36\,\varepsilon^{-2}$	$8.00\,\varepsilon^{-4}$	$2.89\,\varepsilon^{-2}$	$1.33\,\varepsilon^{-1}$	$1.70\,\varepsilon^{-1}$
	ALO [24]	$-9.24\,\varepsilon^{-1}$	$2.76\,\varepsilon^{-3}$	$5.94\,\varepsilon^{-5}$	$-1.91\,\varepsilon^{-4}$	$1.76\,\varepsilon^{+1}$	$1.36\,\varepsilon^{-2}$	$2.67\,\varepsilon^{-4}$	$2.94\,\varepsilon^{-2}$	$1.33\,\varepsilon^{-1}$	$1.72\,\varepsilon^{-1}$
	HCLAOA [20]	−1.05	$3.14\,\varepsilon^{-3}$	$6.09\,\varepsilon^{-5}$	$-1.45\,\varepsilon^{-4}$	$2.01\,\varepsilon^{+1}$	$4.41\,\varepsilon^{-2}$	$4.79\,\varepsilon^{-4}$	$8.88\,\varepsilon^{-1}$	$6.10\,\varepsilon^{-1}$	$7.47\,\varepsilon^{-1}$
BCS 500 W—Model	Proposed HCLBES	−1.03	$2.97\,\varepsilon^{-3}$	$7.71\,\varepsilon^{-5}$	$-1.31\,\varepsilon^{-4}$	$2.25\,\varepsilon^{+1}$	$2.17\,\varepsilon^{-2}$	$8.00\,\varepsilon^{-4}$	$6.74\,\varepsilon^{-3}$	$6.57\,\varepsilon^{-2}$	$8.21\,\varepsilon^{-2}$
	ASO	$-9.90\,\varepsilon^{-1}$	$2.65\,\varepsilon^{-3}$	$6.24\,\varepsilon^{-5}$	$-1.27\,\varepsilon^{-4}$	$1.84\,\varepsilon^{+1}$	$2.30\,\varepsilon^{-2}$	$1.28\,\varepsilon^{-4}$	$1.11\,\varepsilon^{-2}$	$8.07\,\varepsilon^{-2}$	$9.66\,\varepsilon^{-2}$
	HHO	−1.12	$3.07\,\varepsilon^{-3}$	$6.36\,\varepsilon^{-5}$	$-1.28\,\varepsilon^{-4}$	$1.76\,\varepsilon^{+1}$	$2.00\,\varepsilon^{-2}$	$1.75\,\varepsilon^{-4}$	$8.08\,\varepsilon^{-3}$	$6.97\,\varepsilon^{-2}$	$8.54\,\varepsilon^{-2}$
	GWO	−1.02	$2.77\,\varepsilon^{-3}$	$6.49\,\varepsilon^{-5}$	$-1.33\,\varepsilon^{-4}$	$2.01\,\varepsilon^{+1}$	$2.20\,\varepsilon^{-2}$	$3.21\,\varepsilon^{-4}$	$6.85\,\varepsilon^{-3}$	$6.53\,\varepsilon^{-2}$	$8.27\,\varepsilon^{-2}$
	SSA	−1.03	$2.73\,\varepsilon^{-3}$	$5.80\,\varepsilon^{-5}$	$-1.30\,\varepsilon^{-4}$	$1.93\,\varepsilon^{+1}$	$2.01\,\varepsilon^{-2}$	$4.22\,\varepsilon^{-4}$	$6.93\,\varepsilon^{-3}$	$6.64\,\varepsilon^{-2}$	$8.33\,\varepsilon^{-2}$
	BES	$-9.93\,\varepsilon^{-1}$	$2.95\,\varepsilon^{-3}$	$8.31\,\varepsilon^{-5}$	$-1.32\,\varepsilon^{-4}$	$2.16\,\varepsilon^{+1}$	$2.17\,\varepsilon^{-2}$	$6.65\,\varepsilon^{-4}$	$6.78\,\varepsilon^{-3}$	$6.58\,\varepsilon^{-2}$	$8.22\,\varepsilon^{-2}$
	WSO [23]	−1.01	$2.42\,\varepsilon^{-3}$	$4.15\,\varepsilon^{-5}$	$-1.31\,\varepsilon^{-4}$	$2.25\,\varepsilon^{+1}$	$2.18\,\varepsilon^{-2}$	$8.00\,\varepsilon^{-4}$	$6.74\,\varepsilon^{-3}$	$6.57\,\varepsilon^{-2}$	$8.21\,\varepsilon^{-2}$
	MVO [22]	−1.02	$2.87\,\varepsilon^{-3}$	$7.08\,\varepsilon^{-5}$	$-1.31\,\varepsilon^{-4}$	$1.96\,\varepsilon^{+1}$	$2.04\,\varepsilon^{-2}$	$3.98\,\varepsilon^{-4}$	$6.95\,\varepsilon^{-3}$	$6.90\,\varepsilon^{-2}$	$8.70\,\varepsilon^{-2}$
	VSDE [46]	−1.08	$3.03\,\varepsilon^{-3}$	$6.91\,\varepsilon^{-5}$	$-1.31\,\varepsilon^{-4}$	$2.15\,\varepsilon^{+1}$	$2.16\,\varepsilon^{-2}$	$6.57\,\varepsilon^{-4}$	$6.81\,\varepsilon^{-3}$	$6.60\,\varepsilon^{-2}$	$8.24\,\varepsilon^{-2}$
	HBO [25]	−1.11	$3.38\,\varepsilon^{-3}$	$8.86\,\varepsilon^{-5}$	$-1.32\,\varepsilon^{-4}$	$2.24\,\varepsilon^{+1}$	$2.20\,\varepsilon^{-2}$	$7.52\,\varepsilon^{-4}$	$6.77\,\varepsilon^{-3}$	$6.57\,\varepsilon^{-2}$	$8.22\,\varepsilon^{-2}$
	ALO [24]	$-9.90\,\varepsilon^{-1}$	$2.51\,\varepsilon^{-3}$	$5.16\,\varepsilon^{-5}$	$-1.31\,\varepsilon^{-4}$	$1.88\,\varepsilon^{+1}$	$2.03\,\varepsilon^{-2}$	$2.91\,\varepsilon^{-4}$	$6.84\,\varepsilon^{-3}$	$6.62\,\varepsilon^{-2}$	$8.28\,\varepsilon^{-2}$
	HCLAOA [20]	−1.04	$2.96\,\varepsilon^{-3}$	$6.29\,\varepsilon^{-5}$	$-1.50\,\varepsilon^{-4}$	$2.21\,\varepsilon^{+1}$	$4.81\,\varepsilon^{-2}$	$5.08\,\varepsilon^{-4}$	1.42	$7.89\,\varepsilon^{-1}$	$9.11\,\varepsilon^{-1}$

Scientific notation ε^n refers to 1×10^n, where n is a real integer value.

Table 9. Statistical analysis of the proposed HCLBES and other algorithms for the PEMFC 500 W model under different operating conditions.

	Algorithm	Best	Worst	Aver	Median	Var	Std
NedStack PS6—Model	Proposed HCLBES	$7.12\,\varepsilon^{-2}$	$7.13\,\varepsilon^{-2}$	$7.12\,\varepsilon^{-2}$	$7.12\,\varepsilon^{-2}$	$2.96\,\varepsilon^{-10}$	$1.72\,\varepsilon^{-5}$
	ASO	$8.30\,\varepsilon^{-2}$	$1.87\,\varepsilon^{-1}$	$1.26\,\varepsilon^{-1}$	$1.27\,\varepsilon^{-1}$	$7.58\,\varepsilon^{-4}$	$2.75\,\varepsilon^{-2}$
	HHO	$7.17\,\varepsilon^{-2}$	$8.69\,\varepsilon^{-2}$	$7.38\,\varepsilon^{-2}$	$7.28\,\varepsilon^{-2}$	$1.26\,\varepsilon^{-5}$	$3.54\,\varepsilon^{-3}$
	GWO	$7.13\,\varepsilon^{-2}$	$8.29\,\varepsilon^{-2}$	$7.49\,\varepsilon^{-2}$	$7.36\,\varepsilon^{-2}$	$1.49\,\varepsilon^{-5}$	$3.85\,\varepsilon^{-3}$
	SSA	$7.12\,\varepsilon^{-2}$	$1.12\,\varepsilon^{-1}$	$8.21\,\varepsilon^{-2}$	$7.60\,\varepsilon^{-2}$	$1.43\,\varepsilon^{-4}$	$1.20\,\varepsilon^{-2}$
	BES	$7.12\,\varepsilon^{-2}$	$7.81\,\varepsilon^{-2}$	$7.23\,\varepsilon^{-2}$	$7.21\,\varepsilon^{-2}$	$1.99\,\varepsilon^{-6}$	$1.41\,\varepsilon^{-3}$
Horizon 500—Model	Proposed HCLBES	$2.89\,\varepsilon^{-2}$	$2.89\,\varepsilon^{-2}$	$2.89\,\varepsilon^{-2}$	$2.89\,\varepsilon^{-2}$	$5.33\,\varepsilon^{-19}$	$7.30\,\varepsilon^{-10}$
	ASO	$3.14\,\varepsilon^{-2}$	$4.84\,\varepsilon^{-2}$	$3.86\,\varepsilon^{-2}$	$3.84\,\varepsilon^{-2}$	$2.39\,\varepsilon^{-5}$	$4.89\,\varepsilon^{-3}$
	HHO	$2.98\,\varepsilon^{-2}$	$8.83\,\varepsilon^{-2}$	$3.63\,\varepsilon^{-2}$	$3.03\,\varepsilon^{-2}$	$3.35\,\varepsilon^{-4}$	$1.83\,\varepsilon^{-2}$
	GWO	$2.90\,\varepsilon^{-2}$	$2.95\,\varepsilon^{-2}$	$2.92\,\varepsilon^{-2}$	$2.90\,\varepsilon^{-2}$	$5.91\,\varepsilon^{-8}$	$2.43\,\varepsilon^{-4}$
	SSA	$2.90\,\varepsilon^{-2}$	$2.95\,\varepsilon^{-2}$	$2.92\,\varepsilon^{-2}$	$2.91\,\varepsilon^{-2}$	$4.24\,\varepsilon^{-8}$	$2.06\,\varepsilon^{-4}$
	BES	$2.89\,\varepsilon^{-2}$	$2.90\,\varepsilon^{-2}$	$2.90\,\varepsilon^{-2}$	$2.89\,\varepsilon^{-2}$	$3.45\,\varepsilon^{-10}$	$1.86\,\varepsilon^{-5}$
BCS 500 W—Model	Proposed HCLBES	$6.74\,\varepsilon^{-3}$	$6.74\,\varepsilon^{-3}$	$6.74\,\varepsilon^{-3}$	$6.74\,\varepsilon^{-3}$	$4.90\,\varepsilon^{-13}$	$7.00\,\varepsilon^{-7}$
	ASO	$6.83\,\varepsilon^{-3}$	$2.10\,\varepsilon^{-2}$	$1.11\,\varepsilon^{-2}$	$9.78\,\varepsilon^{-3}$	$2.29\,\varepsilon^{-5}$	$4.78\,\varepsilon^{-3}$
	HHO	$6.88\,\varepsilon^{-3}$	$1.63\,\varepsilon^{-2}$	$8.08\,\varepsilon^{-3}$	$6.91\,\varepsilon^{-3}$	$8.63\,\varepsilon^{-6}$	$2.94\,\varepsilon^{-3}$
	GWO	$6.77\,\varepsilon^{-3}$	$7.11\,\varepsilon^{-3}$	$6.85\,\varepsilon^{-3}$	$6.81\,\varepsilon^{-3}$	$1.07\,\varepsilon^{-8}$	$1.04\,\varepsilon^{-4}$
	SSA	$6.77\,\varepsilon^{-3}$	$7.26\,\varepsilon^{-3}$	$6.93\,\varepsilon^{-3}$	$6.90\,\varepsilon^{-3}$	$2.59\,\varepsilon^{-8}$	$1.61\,\varepsilon^{-4}$
	BES	$6.75\,\varepsilon^{-3}$	$6.82\,\varepsilon^{-3}$	$6.78\,\varepsilon^{-3}$	$6.77\,\varepsilon^{-3}$	$5.63\,\varepsilon^{-10}$	$2.37\,\varepsilon^{-5}$

Scientific notation ε^n refers to 1×10^n, where n is a real integer value.

In contrast, ASO demonstrates slower convergence and higher final error, indicating suboptimal performance. The results affirm the superior optimization capability and robustness of HCLBES for tuning fuel cell parameters.

Furthermore, Figure 7 illustrates the polarization curves derived from experimental and modelled data for all three PEMFCs. The results demonstrate a strong correlation between the experimental observations and the curves predicted by the proposed HCLBES-identified parameters. The close match between the estimated and actual data for the NedStack PS6, Horizon 500, and BCS 500 W fuel cells at various operating levels shows that the fuel cell-model can accurately predict performance. This consistent alignment points out the importance of proposed HCLBES for reliable performance prediction and optimization in PEMFC models.

Based on comprehensive analysis and performance evaluation, HCLBES is recommended as the most effective search algorithm for the accurate identification of PEMFC model parameters in both 250 W and 500 W configurations.

6.3. Computational Time Analysis

This subsection evaluates the computational efficiency of the proposed optimization algorithm and its counterparts applied for parameter estimation for PEMFC models. Figure 8 shows the computational times required by each algorithm for the two fuel cell configurations. The results show remarkable contrasts in execution time among the studied algorithms. For the PEMFC 250 W models, the HCLBES, while it achieved high estimation accuracy as discussed earlier, requires the longest computation time, exceeding 35 s in some cases.

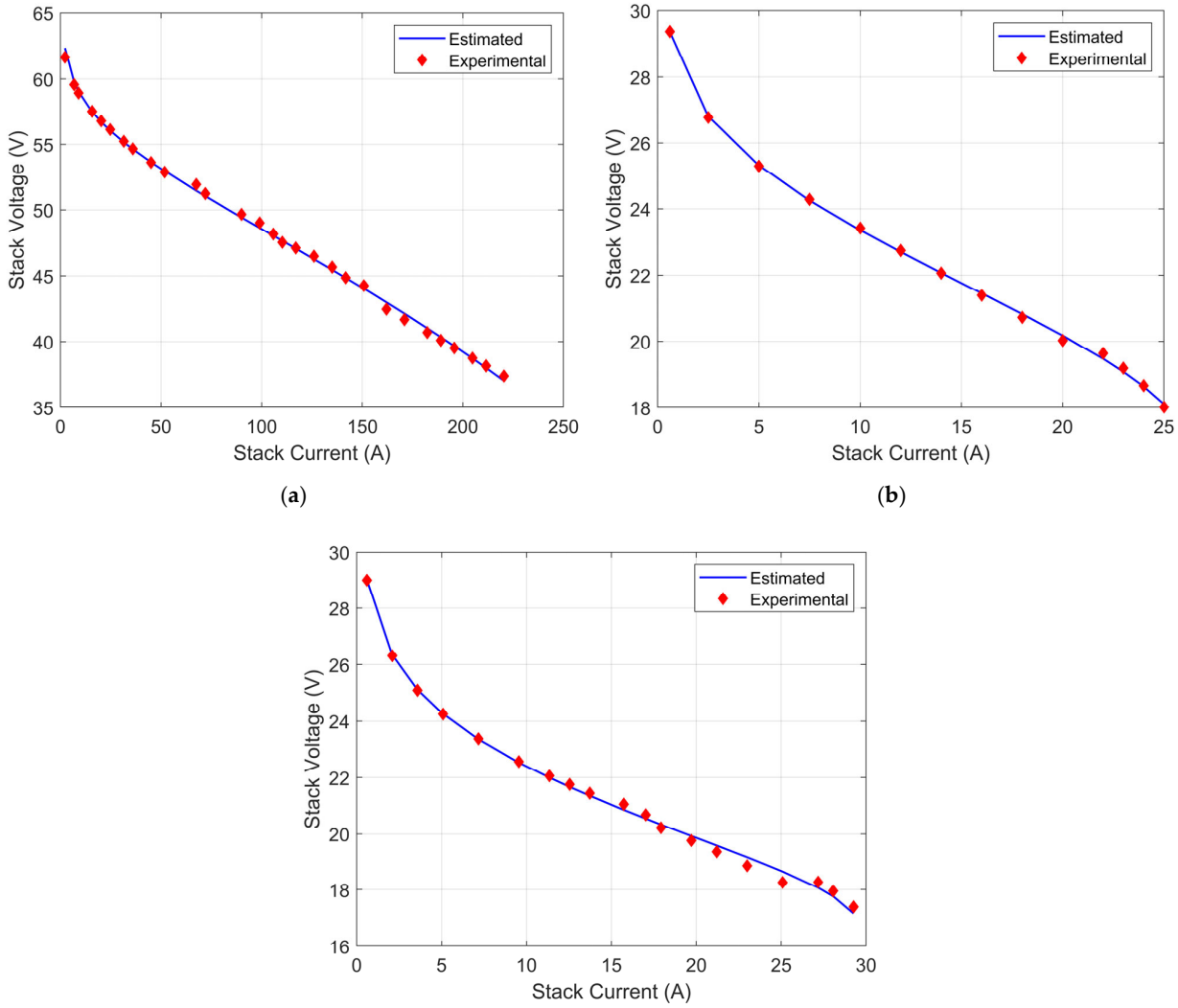


Figure 7. The current-voltage characteristics of the PEMFC models using the HCLBES for (**a**) NedStack PS6 fuel cell, (**b**) Horizon 500 fuel cell, and (**c**) BCS 500 W fuel cell.

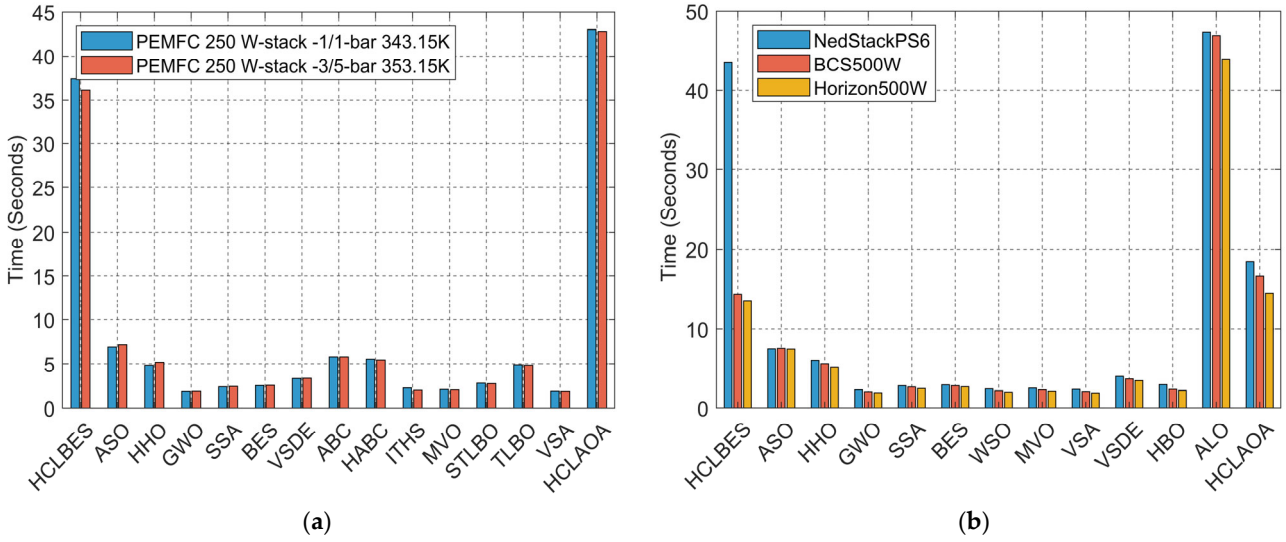


Figure 8. Comparison of computational times required by each optimization algorithm for parameter estimation of the considered PEMFC models: (**a**) PEMFC 250 W and (**b**) PEMFC 500 W (NedStack PS6, BSC500 W, and Horizon 500 W).

Similarly, the HCLAOA algorithm also indicates a comparably high computational time. On the other hand, algorithms like GWO, SSA, and BES reach the minimum convergence point in less than 5 s. A similar trend is observed for the PEMFC 500 W models, where comprehensive search algorithms HCLBES and HCLAOA again record the longest execution times, while other search algorithms maintain minimal computational overhead. Moreover, it is observable that computational time generally scales with fuel cell model stack complexity and the number of experimental points recorded. For most search algorithms, the 500 W configurations require slightly longer times compared to their 250 W counterparts. However, the ranking of the other algorithms remains largely consistent with the 250 W PEMFC models. The increasing number of experimental data points used in most search algorithms leads to increases in computation times, but this does not impact their relative performance order.

Although the proposed HCLBES algorithm demands the longest computation time, it achieves superior parameter estimation performance, which can be explained by its benefit in applications that prefer the accuracy of the estimated parameter over speed.

In addition to that, Table 10 presents a comparative analysis of statistical metrics for execution time. These comparative results indicate that the HCLBES algorithm consistently achieved more effective optimization outcomes than the benchmark metaheuristic algorithms across all studied PEMFC operating conditions. For both PEMFC models, low-power and high-power configurations, HCLBES obtained the best run index of 1 out of 30 runs, demonstrating its ability to reach near-optimal solutions under various thermal and pressure settings.

Table 10. Comparison of statistical metrics of execution time for studied optimization algorithms in PEMFC modeling under 30 independent executions.

Algorithm	PEMFC 250 W						PEMFC 5000 W								
	1/1-Bar 343.15 K			3/5-Bar 343.15 K			NedStack PS6			BSC500 W			Horizon 500 W		
	Aver	**Std**	***ð***	**Aver**	**Std**	***ð***	**Aver**	**Std**	***ð***	**Aver**	**Std**	***ð***	**Aver**	**Std**	***ð***
Proposed HCLBES	46.45	26.44	1	38.49	21.91	1	60.33	34.95	1	14.61	7.83	1	17.10	9.24	1
ASO	8.68	0.91	16	7.18	0.32	29	8.76	0.57	28	7.50	0.20	3	9.31	1.20	1
HHO	5.76	0.25	14	4.86	0.04	7	6.06	0.25	1	5.56	0.04	6	6.60	0.81	2
GWO	2.25	0.18	19	1.85	0.04	11	2.39	0.31	3	2.09	0.03	4	2.32	0.10	9
SSA	3.34	0.32	9	2.39	0.08	11	2.80	0.04	14	2.64	0.05	3	2.90	0.17	4
BES	3.70	0.20	10	2.48	0.04	22	2.98	0.07	6	2.79	0.12	8	3.13	0.17	9

Note: ð denotes the run number in which the algorithm achieved the minimum execution time out of 30 independent runs.

Although the algorithm recorded relatively high average values across all test scenarios, it also exhibited larger standard deviations compared to the counterpart algorithms, suggesting a higher degree of result dispersion among multiple executions. This variation is indicative of the stochastic nature of HCLBES, which emphasizes broad search behaviours and exploration of the solution space rather than premature convergence. The performance patterns reveal that the hybrid structure of the HCLBES algorithm effectively balances global exploration with local refinement. This balance is essential when addressing the nonlinear, multi-modal optimization landscape typically observed in PEMFC system modeling. Compared with algorithms such as HHO and GWO, which also demonstrated stable convergence characteristics, HCLBES showed greater adaptability to varying conditions but at the cost of increased variability.

From an engineering perspective, these findings highlight the practical applicability of HCLBES in enhancing the modeling and control of PEMFC models. By achieving consistent

convergence toward efficient operating points, the algorithm can contribute to improved energy management, reduced hydrogen consumption, and extended stack lifespan.

7. Discussion

The proposed HCLBES algorithm for the parameter identification of PEMFCs under various operating conditions and configurations was thoroughly evaluated in this article. The effectiveness of HCLBES was tested by comparing it with counterpart search optimization algorithms for both 250 W and 500 W PEMFC models. The best parameter values for the 250 W PEMFC stack under different conditions, such as pressures of 1/1 bar and temperatures of 343.15 K, as well as 3/5 bar and 353.15 K, are shown in Tables 4 and 5. The results validate that the HCLBES performed better than its counterparts by consistently estimating parameters that led to more accurate representations of PEMFC models. The statistical analyses in Tables 6 and 7 further support this conclusion by demonstrating that HCLBES has superior optimization capability and significantly lower error metrics (e.g., MSE, RMSE). These results are supported by Figures 4 and 5. Compared to other algorithms, HCLBES achieved faster convergence to the best solutions in fewer iterations and more consistent performance, as shown in the convergence plots in Figure 4. Meanwhile, the current voltage curves in Figure 5 showed that the parameter sets identified by HCLBES produced polarization curves that closely aligned with experimental data in both tested scenarios, with an average deviation below 2%.

These results indicate that the HCLBES algorithm is effective at simulating complex systems like PEMFCs and works well in various situations. Tables 8 and 9, along with Figures 6 and 7, analyze the application of HCLBES to 500 W PEMFC models, which include the NedStack PS6, Horizon 500, and BCS 500 W fuel cells. Once again, the proposed HCLBES regularly showed better convergence speed and modelling accuracy. Statistical measures and visual data patterns show that the proposed HCLBES can easily adapt and scale to different PEMFC setups and brands.

These results are in line with previous studies that emphasize the importance of heterogeneous comprehensive learning approaches in tasks related to global optimization. Because of the nonlinear electrochemical dynamics involved, previous studies have shown that these algorithms are especially useful for negotiating difficult search areas and avoiding the premature convergence challenges commonly encountered in PEMFC modelling. The evolutionary algorithm allowed for good use of resources, and adding comprehensive learning to HCLBES definitely enhanced the ability to explore new options. More generally, the results of this article have important implications for the development of intelligent modelling tools for fuel cell systems. In practical applications, accurate parameter identification enhances predictive control strategies, energy management systems, and general stack performance optimization in addition to model fidelity.

8. Conclusions

This paper presented and verified a novel search algorithm named HCLBES as a reliable optimization technique for parameter identification in PEMFC models. HCLBES showed excellent convergence behaviour, high modelling accuracy, and strong generalization capability through comparative analysis across various optimization algorithms and PEMFC configurations (250-W and 500-W models). The important conclusions include the following:

- Statistical analyses under various temperature and pressure conditions show that HCLBES regularly obtained lower error rates than conventional methods.
- Simulations were conducted on several PEMFC models to evaluate the performance of the proposed HCLBES algorithm.

- The current voltage curves predicted by HCLBES algorithm showed excellent agreement with the experimental data, with an average error below 2% and a low RMSE value.

The integration of heterogeneous learning mechanisms with the exploratory power of bald eagle search to develop the search algorithm named HCLBES results in a robust and dependable tool for optimization in fuel cell modelling. These features make it especially suitable for uses requiring exact dynamic modelling and adaptive control. Future directions may focus on using the HCLBES for other optimization tasks, which might be useful to optimize other fuel cell models or electrochemical energy systems, and it can be extended by coupling with real-time adaptive control systems. Furthermore, future research could explore hybridization with deep learning methods or surrogate modeling approaches to extend HCLBES to complex, data-driven environments. Finally, future directions may include incorporating rigorous statistical significance testing, such as ANOVA or non-parametric methods, across multiple independent runs. This approach could provide a formal assessment of algorithm performance and validate whether improvements over other algorithms are statistically meaningful.

Author Contributions: Conceptualization, methodology, software, and validation A.K.A.; investigation, A.N.H. and A.K.A.; writing—original draft preparation, A.K.A. and M.A.A.-O.; writing—review and editing, M.A.A.-O. and A.K.A.; formal analysis M.A.A.-O.; data curation, supervision, and project administration S.A.-A. and A.N.H. All authors have read and agreed to the published version of the manuscript.

Funding: This research was funded by AL-Naji University, which strives for scientific excellence and supports it.

Institutional Review Board Statement: Not applicable.

Informed Consent Statement: Not applicable.

Data Availability Statement: All sources of data used here are cited in the text or provided in the tables in this paper.

Acknowledgments: The authors gratefully acknowledge the support of Middle Technical University and Al-Naji University, which sponsored this research as part of its commitment to advancing scientific knowledge and fostering academic excellence.

Conflicts of Interest: The authors declare no conflicts of interest.

Nomenclature

A	Active cell area (m^2)
α	Transfer coefficient—(dimensionless)
b	A constant related to concentration voltage drop (V)
CO_2	Oxygen concentration $(mol.m^{-3})$
E_0	Reference voltage (V)
E_{Nernst}	Reversible thermodynamic potential (Nernst-voltage) (V)
e^-	Electrons—(elementary charge)
F	Faraday's constant with numerical value 96486 $C.mol^{-1}$
H_2	Hydrogen gas (mol)
H_2O_2	Water (mol)
H^+	Protons (mol)
I_{cell}	Fuel cell current (A)
J_{cell}	Exchange current density $(A.m^{-2})$
j_{Max}	Maximum current density $(A.m^{-2})$

ℓ	Membrane thickness (m)
N	Number of search agents
n_s	Number of series-connected cells
O_2	Oxygen gas (mol)
PH_2	Partial pressure of hydrogen
PO_2	Partial pressure of oxygen
R	Universal gas constant $\left(\text{Jmol}^{-1}\text{k}^{-1}\right)$
r	Random coefficient
r_M	Membrane resistivity (Ωm)
R_c	Contact resistance to electron conduction (Ω)
T_K	Cell temperature in Kelvin
t	Number of iterations
V_{act}	Activation voltage drops (V)
V_{Con}	Concentration voltage drops (V)
V_{Fc}	Terminal voltage of a PEMFC (V)
V_{ohm}	Ohmic voltage drop (V)
V_{Stack}	Overall voltage of a PEMFC stack (V)
Z	Population of solutions
Z_{best_i}	Optimal search position
$Z_{i,t}$	Current position of the eagle in the search space at iteration t
$Z_{i,t+1}$	Updated position after selection, search, or swooping stage
Z_{mean_i}	Mean position from the previous search
ζ	Number of electrons transferred
$\eta_1, \eta_2, \eta_3, \eta_4$	Empirical coefficients for the activation overpotentials (V)
γ	Reversible (thermodynamic) voltage
β	Activation losses
φ	Ohmic losses
ϵ	Concentration losses
λ	Membrane water content ratio—1 mol (H_2O /$SO^-{}_3$)
ξ	Location update parameter

References

1. Rashid, F.L.; Al-Obaidi, M.A.; Hussein, A.K.; Akkurt, N.; Ali, B.; Younis, O. Floating Solar Stills and Floating Solar-Driven Membranes: Recent Advances and Overview of Designs, Performance and Modern Combinations. *Sol. Energy* **2022**, *247*, 355–372. [CrossRef]
2. Priya, K.; Sathishkumar, K.; Rajasekar, N. A Comprehensive Review on Parameter Estimation Techniques for Proton Exchange Membrane Fuel Cell Modelling. *Renew. Sustain. Energy Rev.* **2018**, *93*, 121–144. [CrossRef]
3. Mirzapour, F.; Lakzaei, M.; Varamini, G.; Teimourian, M.; Ghadimi, N. A New Prediction Model of Battery and Wind-Solar Output in Hybrid Power System. *J. Ambient Intell. Humaniz. Comput.* **2019**, *10*, 77–87. [CrossRef]
4. Gong, W.; Yan, X.; Hu, C.; Wang, L.; Gao, L. Fast and Accurate Parameter Extraction for Different Types of Fuel Cells with Decomposition and Nature-Inspired Optimization Method. *Energy Convers. Manag.* **2018**, *174*, 913–921. [CrossRef]
5. Liu, B.; Chen, H.; Zhang, T.; Pei, P. A Vehicular Proton Exchange Membrane Fuel Cell System Co-Simulation Modeling Method Based on the Stack Internal Distribution Parameters Monitoring. *Energy Convers. Manag.* **2019**, *197*, 111898. [CrossRef]
6. Bankupalli, P.T.; Ghosh, S.; Kumar, L.; Samanta, S.; Dixit, T.V. A Non-Iterative Approach for Maximum Power Extraction from PEM Fuel Cell Using Resistance Estimation. *Energy Convers. Manag.* **2019**, *187*, 565–577. [CrossRef]
7. Stepančič, M.; Juričić, Đ.; Boškoski, P. Fault Detection of Fuel Cell Systems Based on Statistical Assessment of Impedance Data. *Energy Convers. Manag.* **2019**, *195*, 76–85. [CrossRef]
8. Su, C.; Xu, Z.; Wang, X.; Li, B. Research on the Co-Evolution Mechanism of Electricity Market Entities Enabled by Shared Energy Storage: A Tripartite Game Perspective Incorporating Dynamic Incentives/Penalties and Stochastic Disturbances. *Systems* **2025**, *13*, 817. [CrossRef]
9. Yang, S.; Chellali, R.; Lu, X.; Li, L.; Bo, C. Modeling and Optimization for Proton Exchange Membrane Fuel Cell Stack Using Aging and Challenging P Systems Based Optimization Algorithm. *Energy* **2016**, *109*, 569–577. [CrossRef]
10. Ettihir, K.; Boulon, L.; Becherif, M.; Agbossou, K.; Ramadan, H.S. Online Identification of Semi-Empirical Model Parameters for PEMFCs. *Int. J. Hydrogen Energy* **2014**, *39*, 21165–21176. [CrossRef]

11. Amphlett, J.C.; Baumert, R.M.; Mann, R.F.; Peppley, B.A.; Roberge, P.R.; Harris, T.J. Performance Modeling of the Ballard Mark IV Solid Polymer Electrolyte Fuel Cell: II. Empirical Model Development. *J. Electrochem. Soc.* **1995**, *142*, 9–15. [CrossRef]
12. Saadi, A.; Becherif, M.; Aboubou, A.; Ayad, M.Y. Comparison of Proton Exchange Membrane Fuel Cell Static Models. *Renew. Energy* **2013**, *56*, 64–71. [CrossRef]
13. Kandidayeni, M.; Macias, A.; Khalatbarisoltani, A.; Boulon, L.; Kelouwani, S. Benchmark of Proton Exchange Membrane Fuel Cell Parameters Extraction with Metaheuristic Optimization Algorithms. *Energy* **2019**, *183*, 912–925. [CrossRef]
14. Priya, K.; Sudhakar Babu, T.; Balasubramanian, K.; Sathish Kumar, K.; Rajasekar, N. A Novel Approach for Fuel Cell Parameter Estimation Using Simple Genetic Algorithm. *Sustain. Energy Technol. Assess.* **2015**, *12*, 46–52. [CrossRef]
15. Zhang, L.; Wang, N. An Adaptive RNA Genetic Algorithm for Modeling of Proton Exchange Membrane Fuel Cells. *Int. J. Hydrogen Energy* **2013**, *38*, 219–228. [CrossRef]
16. Mo, Z.J.; Zhu, X.J.; Wei, L.Y.; Cao, G.Y. Parameter Optimization for a PEMFC Model with a Hybrid Genetic Algorithm. *Int. J. Energy Res.* **2006**, *30*, 585–597. [CrossRef]
17. Ohenoja, M.; Leiviskä, K. Validation of Genetic Algorithm Results in a Fuel Cell Model. *Int. J. Hydrogen Energy* **2010**, *35*, 12618–12625. [CrossRef]
18. Askarzadeh, A.; Rezazadeh, A. A New Artificial Bee Swarm Algorithm for Optimization of Proton Exchange Membrane Fuel Cell Model Parameters. *J. Zhejiang Univ. Sci. C* **2011**, *12*, 638–646. [CrossRef]
19. Askarzadeh, A.; Rezazadeh, A. Artificial Immune System-Based Parameter Extraction of Proton Exchange Membrane Fuel Cell. *Int. J. Electr. Power Energy Syst.* **2011**, *33*, 933–938. [CrossRef]
20. Al-Hotmani, O.M.A.; Al-Obaidi, M.A.; Li, J.P.; John, Y.M.; Patel, R.; Mujtaba, I.M. A Multi-Objective Optimisation Framework for MED-TVC Seawater Desalination Process Based on Particle Swarm Optimisation. *Desalination* **2022**, *525*, 115504. [CrossRef]
21. Al-Obaidi, M.; Li, J.-P.; Alsadaie, S.; Kara-Zaïtri, C.; Mujtaba, I. Modelling and Optimisation of a Multistage Reverse Osmosis Processes with Permeate Reprocessing and Recycling for the Removal of N-Nitrosodimethylamine from Wastewater Using Species Conserving Genetic Algorithms. *Chem. Eng. J.* **2018**, *37*, 735–760. [CrossRef]
22. Fathy, A.; Babu, T.S.; Abdelkareem, M.A.; Rezk, H.; Yousri, D. Recent Approach Based Heterogeneous Comprehensive Learning Archimedes Optimization Algorithm for Identifying the Optimal Parameters of Different Fuel Cells. *Energy* **2022**, *248*, 123587. [CrossRef]
23. Zhang, W.; Wang, N.; Yang, S. Hybrid Artificial Bee Colony Algorithm for Parameter Estimation of Proton Exchange Membrane Fuel Cell. *Int. J. Hydrogen Energy* **2013**, *38*, 5796–5806. [CrossRef]
24. Fathy, A.; Rezk, H. Multi-Verse Optimizer for Identifying the Optimal Parameters of PEMFC Model. *Energy* **2018**, *143*, 634–644. [CrossRef]
25. Ayyarao, T.S.L.V.; Polumahanthi, N.; Khan, B. An Accurate Parameter Estimation of PEM Fuel Cell Using War Strategy Optimization. *Energy* **2024**, *290*, 130235. [CrossRef]
26. Rao, Y.; Shao, Z.; Ahangarnejad, A.H.; Gholamalizadeh, E.; Sobhani, B. Shark Smell Optimizer Applied to Identify the Optimal Parameters of the Proton Exchange Membrane Fuel Cell Model. *Energy Convers. Manag.* **2019**, *182*, 1–8. [CrossRef]
27. Abdel-Basset, M.; Mohamed, R.; Elhoseny, M.; Chakrabortty, R.K.; Ryan, M.J. An Efficient Heap-Based Optimization Algorithm for Parameters Identification of Proton Exchange Membrane Fuel Cells Model: Analysis and Case Studies. *Int. J. Hydrogen Energy* **2021**, *46*, 11908–11925. [CrossRef]
28. Li, J.; Gao, X.; Cui, Y.; Hu, J.; Xu, G.; Zhang, Z. Accurate, Efficient and Reliable Parameter Extraction of PEM Fuel Cells Using Shuffled Multi-Simplexes Search Algorithm. *Energy Convers. Manag.* **2020**, *206*, 112501. [CrossRef]
29. Rezk, H.; Wilberforce, T.; Olabi, A.G.; Ghoniem, R.M.; Sayed, E.T.; Ali Abdelkareem, M. Optimal Parameter Identification of a PEM Fuel Cell Using Recent Optimization Algorithms. *Energies* **2023**, *16*, 5246. [CrossRef]
30. Xu, S.; Wang, Y.; Wang, Z. Parameter Estimation of Proton Exchange Membrane Fuel Cells Using Eagle Strategy Based on JAYA Algorithm and Nelder-Mead Simplex Method. *Energy* **2019**, *173*, 457–467. [CrossRef]
31. Gong, W.; Yan, X.; Liu, X.; Cai, Z. Parameter Extraction of Different Fuel Cell Models with Transferred Adaptive Differential Evolution. *Energy* **2015**, *86*, 139–151. [CrossRef]
32. Sun, Z.; Wang, N.; Bi, Y.; Srinivasan, D. Parameter Identification of PEMFC Model Based on Hybrid Adaptive Differential Evolution Algorithm. *Energy* **2015**, *90*, 1334–1341. [CrossRef]
33. Askarzadeh, A.; Rezazadeh, A. A Grouping-Based Global Harmony Search Algorithm for Modeling of Proton Exchange Membrane Fuel Cell. *Int. J. Hydrogen Energy* **2011**, *36*, 5047–5053. [CrossRef]
34. El-Fergany, A.A. Electrical Characterisation of Proton Exchange Membrane Fuel Cells Stack Using Grasshopper Optimizer. *IET Renew. Power Gener.* **2018**, *12*, 9–17. [CrossRef]
35. Niu, Q.; Zhang, L.; Li, K. A Biogeography-Based Optimization Algorithm with Mutation Strategies for Model Parameter Estimation of Solar and Fuel Cells. *Energy Convers. Manag.* **2014**, *86*, 1173–1185. [CrossRef]
36. Turgut, O.E.; Coban, M.T. Optimal Proton Exchange Membrane Fuel Cell Modelling Based on Hybrid Teaching Learning Based Optimization—Differential Evolution Algorithm. *Ain Shams Eng. J.* **2016**, *7*, 347–360. [CrossRef]

37. Agwa, A.M.; El-Fergany, A.A.; Sarhan, G.M. Steady-State Modeling of Fuel Cells Based on Atom Search Optimizer. *Energies* **2019**, *12*, 1884. [CrossRef]
38. Chen, Y.; Wang, N. Cuckoo Search Algorithm with Explosion Operator for Modeling Proton Exchange Membrane Fuel Cells. *Int. J. Hydrogen Energy* **2019**, *44*, 3075–3087. [CrossRef]
39. Mirjalili, S.; Gandomi, A.H.; Mirjalili, S.Z.; Saremi, S.; Faris, H.; Mirjalili, S.M. Salp Swarm Algorithm: A Bio-Inspired Optimizer for Engineering Design Problems. *Adv. Eng. Softw.* **2017**, *114*, 163–191. [CrossRef]
40. El-Fergany, A.A. Extracting Optimal Parameters of PEM Fuel Cells Using Salp Swarm Optimizer. *Renew. Energy* **2018**, *119*, 641–648. [CrossRef]
41. Priya, K.; Rajasekar, N. Application of Flower Pollination Algorithm for Enhanced Proton Exchange Membrane Fuel Cell Modelling. *Int. J. Hydrogen Energy* **2019**, *44*, 18438–18449. [CrossRef]
42. El-Fergany, A.A.; Hasanien, H.M.; Agwa, A.M. Semi-Empirical PEM Fuel Cells Model Using Whale Optimization Algorithm. *Energy Convers. Manag.* **2019**, *201*, 112197. [CrossRef]
43. Shehab, M.; Mashal, I.; Momani, Z.; Shambour, M.K.Y.; AL-Badareen, A.; Al-Dabet, S.; Bataina, N.; Alsoud, A.R.; Abualigah, L. Harris Hawks Optimization Algorithm: Variants and Applications. *Arch. Comput. Methods Eng.* **2022**, *29*, 5579–5603. [CrossRef]
44. Rezk, H.; Olabi, A.G.; Ferahtia, S.; Sayed, E.T. Accurate Parameter Estimation Methodology Applied to Model Proton Exchange Membrane Fuel Cell. *Energy* **2022**, *255*, 124454. [CrossRef]
45. Sarkar, J.; Bhattacharyya, S. A New Heuristic Optimization Algorithm for Modeling of Proton Exchange Membrane Fuel Cell: Bird Mating Optimizer. *Arch. Thermodyn.* **2012**, *33*, 23–40. [CrossRef]
46. Mirjalili, S.; Mirjalili, S.M.; Lewis, A. Grey Wolf Optimizer. *Adv. Eng. Softw.* **2014**, *69*, 46–61. [CrossRef]
47. Fathy, A.; Elaziz, M.A.; Alharbi, A.G. A Novel Approach Based on Hybrid Vortex Search Algorithm and Differential Evolution for Identifying the Optimal Parameters of PEM Fuel Cell. *Renew. Energy* **2020**, *146*, 1833–1845. [CrossRef]
48. Guo, C.; Lu, J.; Tian, Z.; Guo, W.; Darvishan, A. Optimization of Critical Parameters of PEM Fuel Cell Using TLBO-DE Based on Elman Neural Network. *Energy Convers. Manag.* **2019**, *183*, 149–158. [CrossRef]
49. Fawzi, M.; El-Fergany, A.A.; Hasanien, H.M. Effective Methodology Based on Neural Network Optimizer for Extracting Model Parameters of PEM Fuel Cells. *Int. J. Energy Res.* **2019**, *43*, 8136–8147. [CrossRef]
50. Kandidayeni, M.; Macias, A.; Amamou, A.A.; Boulon, L.; Kelouwani, S.; Chaoui, H. Overview and Benchmark Analysis of Fuel Cell Parameters Estimation for Energy Management Purposes. *J. Power Sources* **2018**, *380*, 92–104. [CrossRef]
51. Rathod, A.A.; Sharma, P.; Choudhary, A.; Raju, S.; Subramanian, B. An Efficient Framework for Proton Exchange Membrane Fuel Cell Parameter Estimation Using Numerous MH Algorithms. *Renew. Sustain. Energy Rev.* **2025**, *216*, 115603. [CrossRef]
52. Amphlett, J.C.; Baumert, R.M.; Mann, R.F.; Peppley, B.A.; Roberge, P.R.; Rodrigues, A. Parametric Modelling of the Performance of a 5-KW Proton-Exchange Membrane Fuel Cell Stack. *J. Power Sources* **1994**, *49*, 349–356. [CrossRef]
53. Squadrito, G.; Maggio, G.; Passalacqua, E.; Lufrano, F.; Patti, A. Empirical Equation for Polymer Electrolyte Fuel Cell (PEFC) Behaviour. *J. Appl. Electrochem.* **1999**, *29*, 1449–1455. [CrossRef]
54. Rowe, A.; Li, X. Mathematical Modeling of Proton Exchange Membrane Fuel Cells. *J. Power Sources* **2001**, *102*, 82–96. [CrossRef]
55. Alsattar, H.A.; Zaidan, A.A.; Zaidan, B.B. Novel Meta-Heuristic Bald Eagle Search Optimisation Algorithm. *Artif. Intell. Rev.* **2020**, *53*, 2237–2264. [CrossRef]
56. Niu, Q.; Zhang, H.; Li, K. An Improved TLBO with Elite Strategy for Parameters Identification of PEM Fuel Cell and Solar Cell Models. *Int. J. Hydrogen Energy* **2014**, *39*, 3837–3854. [CrossRef]
57. Yadav, P.; Kumar, R.; Panda, S.K.; Chang, C.S. An Intelligent Tuned Harmony Search Algorithm for Optimisation. *Inf. Sci.* **2012**, *196*, 47–72. [CrossRef]
58. Liang, J.J.; Qin, A.K.; Suganthan, P.N.; Baskar, S. Comprehensive Learning Particle Swarm Optimizer for Global Optimization of Multimodal Functions. *IEEE Trans. Evol. Comput.* **2006**, *10*, 281–295. [CrossRef]

Disclaimer/Publisher's Note: The statements, opinions and data contained in all publications are solely those of the individual author(s) and contributor(s) and not of MDPI and/or the editor(s). MDPI and/or the editor(s) disclaim responsibility for any injury to people or property resulting from any ideas, methods, instructions or products referred to in the content.